QTAIM-Based Comparison of Agostic Bonds and Intramolecular Charge-Inverted Hydrogen Bonds

ARTICLE *in* THE JOURNAL OF PHYSICAL CHEMISTRY A · APRIL 2015

Impact Factor: 2.69 · DOI: 10.1021/acs.jpca.5b02041 · Source: PubMed

1 AUTHOR:

Miroslaw Jablonski

Nicolaus Copernicus University

29 PUBLICATIONS **436** CITATIONS

SEE PROFILE

THE JOURNAL OF PHYSICAL CHEMISTRY A

Article

pubs.acs.org/JPCA

QTAIM-Based Comparison of Agostic Bonds and Intramolecular Charge-Inverted Hydrogen Bonds

Mirosław Jabłoński*

Department of Quantum Chemistry, Faculty of Chemistry, Nicolaus Copernicus University in Toruń, 7-Gagarina St., PL-87 100 Toruń, Poland

ABSTRACT: Using DFT-based calculations with seven exchange−correlation functionals (BP86, B3LYP, B3PW91, PBE0, TPSSh, M06-L, M06) we have performed comparative studies on α-, β-, γ-, and δ-agostic bonds (ABs) and intramolecular charge-inverted hydrogen bonds (IMCIHBs). Our detailed analysis of values of QTAIM parameters computed at bond (BCP) and ring critical points (RCP) as well as of the curvatures of bond paths tracing agostic bonds and intramolecular charge-inverted hydrogen bonds gives the opportunity to distinguish between both these types of interactions. In the case of molecules with agostic bonds, the BCP is significantly closer to the agostic hydrogen, whereas in systems with IMCIHB the BCP is, instead, somewhat closer to the metal atom. Agostic bonds are characterized by H···M bond paths being straight in the BCP···M section and then highly curved near the agostic hydrogen, whereas in the case of IMCIHB any substantial curvature of BP in the vicinity of hydrogen is not present. Quite the contrary, the significant curvature of BP near the metal atom can be obtained, instead. One can also distinguish IMCIHBs and ABs on the basis of values of bond ellipticity at BCP and the electron density at RCP which are either somewhat (PBE0) or considerably (M06) greater for the latter type of interaction. It has also been shown that, in general, the exchange−correlation functional has small influences on most of QTAIM parameters computed at BCP and RCP. More significant influences have only been obtained for Laplacian of the electron density, some its components, and the bond ellipticity.

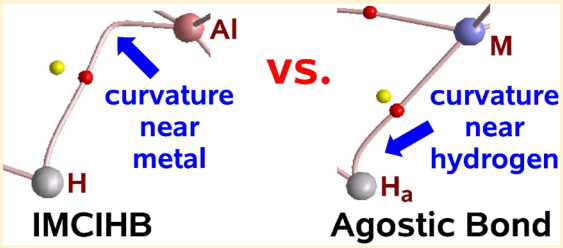

INTRODUCTION

Very recently we have performed[1] ab initio calculations for a wide range of systems possessing various types of interactions involving a partially negatively charged hydrogen atom, i.e., a hydridic hydrogen. As a result, we have shown that charge-inverted hydrogen bond (CIHB)[1−6] is a new type of interaction. Particular attention has been paid to the theoretical comparison of systems with intramolecular charge-inverted hydrogen bond (IMCIHB)[3,4] and agostic bond (AB).[7−16] Some important differences between IMCIHB and AB have already been exposed[1] on the basis of formal definitions of both these types of interactions. Namely, whereas in the case of CIHB, which can be labeled as $X^{\delta+}-H^{\delta-}\cdots Y$, X can be any atom less electronegative than H and Y can be any atom possessing an electron lone-pair vacancy,[2] in the case of an agostic bond, on the contrary, the X−H unit is to be situated in such a way that both X and H atoms are in a close proximity to Y, thus forming an (X−H)···Y interaction.[14−16] Although nowadays one can find numerous literature cases where X = Si or B[14,16−18] and Y ≠ M (M = transition metal)[14,19−21] or even where the agostic hydrogen is replaced by another atom,[22] it should be recalled that the term agostic was introduced to refer to (C−H)···M interactions only,[7−9] i.e., interactions where X = C and Y = M. It also should be mentioned that according to the IUPAC Gold Book,[23] the presence of a coordinatively unsaturated metal atom is still considered as the necessary factor to define the agostic bond. Importantly, the agostic bond is in fact an intramolecular interaction;[14,16] therefore, from this reason, it seems to be more proper to compare AB with IMCIHB rather than with CIHB.[1]

Taking, however, into account "wider definitions" of an agostic bond, where neither X has to be necessarily carbon nor, additionally, Y has to be a transition metal, it might have seemed that the Si−H···Al charge-inverted hydrogen bond found earlier[3,4] in several systems is an example of an agostic bond. Thus, for a proper classification of charge-inverted hydrogen bonds, it is necessary to study similarities (if any) and differences between IMCIHBs and ABs. In the case of agostic bonds, however, it is far more properly to relate to a more standard case, i.e., to systems possessing a (C−H)···M interaction.

Some other important differences between these two types of interactions have recently been reported[1] on the basis of QTAIM[24−26] calculations. Our preliminary studies have shown that, as it seems to be so far the most important finding, an agostic bond in general features a highly curved H···M bond path (BP) with its curvature being near the agostic hydrogen, whereas IMCIHB forms a rather straight H···Al bond path. Moreover, in one case, where this bond path has been found to be curved, the curvature of BP has been found to be located near the aluminum atom.[1] Also, it seems that, in the case of agostic bonds, values of the electron density (ρ_b) and its

Received: March 2, 2015
Revised: April 22, 2015
Published: April 22, 2015

DOI: 10.1021/acs.jpca.5b02041
J. Phys. Chem. A 2015, 119, 4993−5008

Laplacian ($\nabla^2\rho_b$) computed at a bond critical point[24−26] are both larger than in the case of intramolecular charge-inverted hydrogen bonds.[1]

For systems with IMCIHB the above-mentioned findings have resulted from B3LYP/aug-cc-pVTZ calculations, whereas different exchange−correlation functionals and basis sets have been used in cited references referring to QTAIM results for agostic bonds.[27−30] Moreover, we are aware that, in general, values of ρ_b and, in particular, of $\nabla^2\rho_b$ (also its sign) may depend on the choice of the exchange−correlation functional in the case of DFT-based calculations.[31,32] In the case of our calculations, values of ρ_b and $\nabla^2\rho_b$ as well as components of the latter will be important QTAIM parameters; thus the possibility of their dependence on the functional should be considered. Even more importantly, it has been shown[32] that the choice of the exchange−correlation functional may have some impact on a molecular graph. In the case of molecular graphs for complexes possessing agostic bonds it may lead (see, e.g., Figure 6 in ref 32) to different bond paths, e.g., M···H_a if one functional is used, whereas M···C_a if another. This possibility partly results from differences in molecular geometries that can be obtained by means of various DFT functionals.[33−35] Because our studies are to be based on molecular graphs and in particular on the presence of H···M/Al bond paths, the ability to create a bond path to a carbon instead of to the agostic hydrogen was taken into account. It turned out, however, that our model systems reveal agostic bonds that are "stable" with respect to the permanent presence of the M···H_a bond path irrespective of the choice of the exchange−correlation functional. This makes our comparison between agostic bonds and intramolecular charge-inverted hydrogen bonds more reliable. See the Systems section for a full characterization of our model systems possessing either an agostic bond or an intramolecular charge-inverted hydrogen bond.

We have used seven DFT functionals: BP86, B3LYP, B3PW91, PBE0, TPSSh, M06-L, M06. Most of them belong to the group of the so-called hybrid exchange−correlation functionals, because there were claimed[32] to yield the best values of QTAIM local parameters in comparison with CCSD results. Both B3LYP and B3PW91 are likely the most often used in theoretical studies of molecular properties due to their general good performance and are often treated as standard in DFT.[36] PBE0 was in the group of the best performing for QTAIM calculations[32] and TPSSh (and TPSS) was shown to give the best geometries of first row transition metal complexes if compared to experimental structures,[33] BP86 was shown by Bühl and Kabrede[33] to perform worse than TPSSh but better than B3LYP. Finally, Zhao and Truhlar have recently recommended M06-L and M06 functionals for transition metals.[37] For more details on computational methods see the Methodology section.

METHODOLOGY

As already mentioned in the Introduction, all calculations (full geometry optimizations and QTAIM-based calculations) have been performed by means of density functional theory (DFT)[38] using seven exchange−correlation functionals: BP86,[39,40] B3LYP,[41,42] B3PW91,[41,43,44] PBE0,[45−47] TPSSh,[48] M06-L,[49] and M06[37]—all but BP86 and M06-L being hybrid functionals that include a mixture of Hartree−Fock exchange with DFT exchange−correlation. The reasoning of their use has been explained at the end of Introduction. Large aug-cc-pVTZ basis set[50,51] has been used to describe all atoms except Ti and Co for which aug-cc-pVDZ basis set[52,53] has been used due to computational limitations in QTAIM calculations. It has been shown recently[54,55] that the aug-cc-pVTZ basis set gives satisfactory values of QTAIM parameters similar to those obtained by the use of larger Dunning-type basis sets. Geometry optimizations and frequency calculations to analyze characters of obtained stationary points have been performed using Gaussian 09 suit of codes.[56] To improve the accuracy of calculations, the pruned (99 590) grid was requested (Integral (UltraFineGrid) command in Gaussian) and convergence criteria for geometry optimizations were additionally tightened (Opt = Tight option). No imaginary frequency has been found, confirming that obtained geometries correspond to local minima on the potential energy hypersurface. Detailed analysis of the topology of the electron density distribution has been made by means of quantum theory of atoms in molecules (QTAIM) proposed by Bader[24−26] using AIM2000 program.[57] Because QTAIM will be the fundamental tool for the comparison of agostic bonds and intramolecular charge-inverted hydrogen bonds, some basic elements of QTAIM are given below.

QTAIM gives the opportunity to divide a molecule (a system) to atoms (subsystems) by means of a physically well-defined bounding surfaces that are established by the electron density gradient vector field ($\vec{\nabla}\rho$). More strictly, these bounding surfaces are established in such a way that there must not be a flux in $\vec{\nabla}\rho$ through them, meaning a balance in the forces that the neighboring nuclei exert on electrons. Thus, a surface satisfying this condition is termed "a zero flux surface". In the case of bonding interatomic contacts, this surface passes through a point called a bond critical point (BCP), where the gradient of the electron density vanishes, $\vec{\nabla}\rho = \vec{0}$, and the electron density is minimal with respect to the direction of a line connecting two nuclei and maximal with respect to all directions perpendicular to this line. Thus, BCP features one positive and two negative curvatures. If a molecule is in the geometry equilibrium state, then the pair of gradient paths connecting the BCP with its neighboring nuclei is termed a bond path (BP). According to Bader[24] the presence of a bond path and a concomitant bond critical point is a necessary and sufficient condition for any two atoms to be bonded to each other. Another type of a critical point is the so-called ring critical point (RCP) that is characterized by two positive and one negative curvatures; the latter in the direction being perpendicular to the plane of a ring.

The matrix of second derivatives of the electron density (i.e., the so-called Hessian matrix) can be diagonalized and then its eigenvalues, λ_i (i = 1, 2, 3), are the curvatures of the electron density. The trace of the Hessian matrix, $\sum_i\lambda_i$, is known as the Laplacian of the electron density and, when computed at a BCP, will be labeled as $\nabla^2\rho_b$. In the case of a BCP the values of λ_1 and λ_2 (where both λ_1 and λ_2 are negative and $|\lambda_1| \geq |\lambda_2|$) define ellipticity, $\varepsilon = \lambda_1/\lambda_2 - 1$, that measures the extent to which the electron density is preferentially accumulated in a given plane containing the BP. Large values of ε may, however, also suggest instability of a molecular structure.[58]

Particular attention is paid to values of local QTAIM parameters computed in a bond critical point because they may characterize a bond of interest. In our studies we will refer to values of the electron density (ρ_b), its Laplacian ($\nabla^2\rho_b$), and the electronic total energy density (H_b) computed at BCP of either H···Al in systems with IMCIHB or H···M (M = Ti, Co) in systems with agostic bond ($BCP_{H\cdots Al}$ and $BCP_{H\cdots M}$,

DOI: 10.1021/acs.jpca.5b02041
J. Phys. Chem. A 2015, 119, 4993−5008

respectively). Also, ellipticities computed at $BCP_{H\cdots Al}$ and $BCP_{H\cdots M}$ will be analyzed for comparative purposes. In addition to these QTAIM parameters computed at BCP, we will also report values of the electron density at the ring critical point (ρ_r). Finally, some parameters describing the curvature of the H···Al/M bond path and the position of BCP on this BP will be used as well (see further in the text for their definitions).

SYSTEMS

Systems with IMCIHB. As already mentioned, because the agostic bond is an intramolecular interaction rather than an intermolecular one,[14,16] investigated model systems with charge-inverted hydrogen bonds also possess their intramolecular instances, i.e., IMCIHBs. Systems with IMCIHBs (in fact molecules **0** and **1** do not possess $BP_{H\cdots Al}$, although some geometrical parameters indicate a track of the Si−H···Al IMCIHB) are shown in Figure 1 and for the simplicity they are

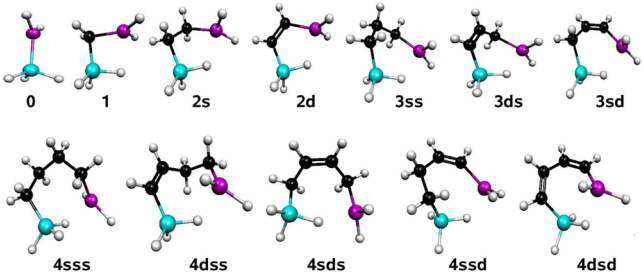

Figure 1. TPSSh-based geometries of investigated model systems with intramolecular charge-inverted hydrogen bond of the Si−H···Al type. Colors of atoms are as follows: H, gray; C, black; Si, blue; Al, magenta.

given labels as follows: (**0**) $H_3Si—AlH_2$, (**1**) $H_3Si—CH_2—AlH_2$, (**2s**) $H_3Si—CH_2—CH_2—AlH_2$, (**2d**) $H_3Si—CH{=}CH—AlH_2$, (**3ss**) $H_3Si—CH_2—CH_2—CH_2—AlH_2$, (**3ds**) $H_3Si—CH{=}CH—CH_2—AlH_2$, (**3sd**) $H_3Si—CH_2—CH{=}CH—AlH_2$, (**4sss**) $H_3Si—CH_2—CH_2—CH_2—CH_2—AlH_2$, (**4dss**) $H_3Si—CH{=}CH—CH_2—CH_2—AlH_2$, (**4sds**) $H_3Si—CH_2—CH{=}CH—CH_2—AlH_2$, (**4ssd**) $H_3Si—CH_2—CH_2—CH{=}CH—AlH_2$, (**4dsd**) $H_3Si—CH{=}CH—CH{=}CH—AlH_2$. The number in the label indicates the number of carbon atoms in the molecular chain and the letter "s" or "d" indicates the formal type (single and double, respectively) of a bond between neighboring carbons if the labeling is started from the silicon.

Systems with Agostic Bond. Particular attention will be given to those agostic systems in which the presence of the agostic bond is indicated not only by geometrical parameters but also by the presence of the H···M bond path. Thus, according to Tognetti et al.,[30] the majority of systems considered in this article contain an agostic bond and not an agostic interaction only. In the latter case the $BP_{H\cdots M}$ would not be present; i.e., the existence of an "agostic bond" would be indicated by appropriate values of some geometrical parameters only. In the case of our studies the presence of $BP_{H\cdots M}$ is, however, crucial because we are going to study the curvature of the H···M bond path. As a consequence, the following set of molecules have been investigated: (**C1EB**) $[Co(Cl_2)Et]^{2+}$, (**C1PG**) $[Co(Cl_2)^nPr]^{2+}$, (**C1BG**) $[Co(Cl_2)^nBu]^{2+}$, (**C1bD**) $[Co(Cl_2)^1Bu]^{2+}$, (**C2MA**) $[CoCp(PH_3)Me]^{+}$, (**C2EA**) and (**C2EB**) $[CoCp(PH_3)Et]^{+}$, (**C2PG**) $[CoCp(PH_3)^nPr]^{+}$, (**T1EB**) $[Ti(Cl_2)Et]^{+}$, (**T2MA**) $TiCp(Cl_2)Me$, and (**T2EA**) $TiCp(Cl_2)Et$, where Me = methyl, Et = ethyl, ^{n}Pr = *n*-propyl, ^{n}Bu = *n*-butyl, ^{1}Bu = 1-butenyl, and Cp = η^5-cyclopentadienyl. The meaning of consecutive letters in **XnYZ** symbol is as follows. **X** being either **C** or **T** indicates the transition metal, Co and Ti, respectively. The number **n** indicates a "class" of a complex, **1** for that with chlorines, **2** for that with Cp. **Y** denotes the type of an alkyl group R: **M** = Me, **E** = Et, **P** = ^{n}Pr, **B** = ^{n}Bu, and **b** = ^{1}Bu. Finally, **Z** indicates the type of an agostic bond: **A** = α, **B** = β, **G** = γ, **D** = δ. Thus, e.g., **C1BG** denotes a cobalt complex of first class (i.e., with two chlorines) possessing ^{n}Bu group forming a γ-agostic bond. As a consequence, the introduced label is both informative (metal, class, alkyl, AB-type) and unique. Note that, although **M** must always be paired with **A** and **P** is paired with **G**, **E** may be paired with either **A** or **B**, and **B** with either **G** or **D**. For complete information, however, we shall be using the **MA** string. As clear from the labels, molecules **C2MA**, **C2EA**, **T2MA**, and **T2EA** possess agostic bonds of α type, **C1EB**, **C2EB**, and **T1EB** possess β-agostic bonds, **C1PG**, **C1BG**, and **C2PG** possess γ-agostic bonds, and molecule **C1bD** features a δ-agostic bond. TPSSh-based geometries of all these molecules are shown in Figure 2.

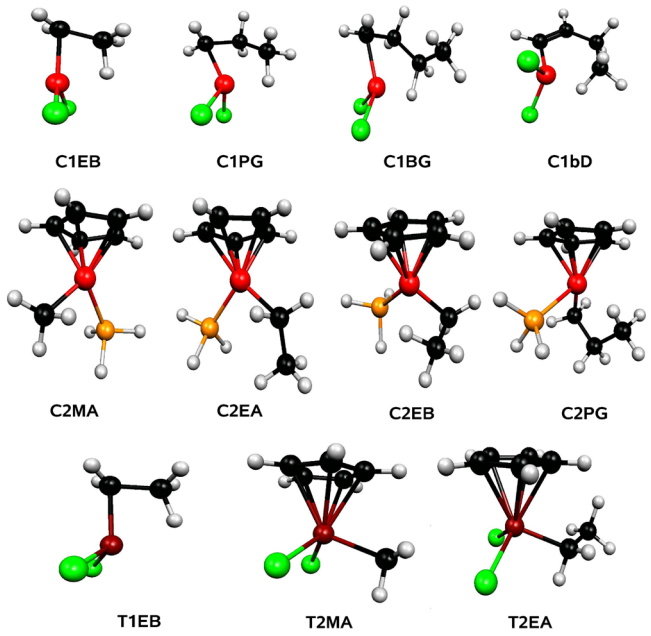

Figure 2. TPSSh-based geometries of investigated model systems with an agostic bond of the M···H type (M = Ti, Co). Colors of atoms are as follows: H, gray; C, black; Cl, green; P, orange; Ti, dark red; Co, light red.

Molecules **T2MA** and **T2EA** will be used to analyze the performance of exchange−correlation functionals used in our study because some geometrical parameters were estimated by Robertson et al.[10] on the basis of infrared spectra. Moreover, they reported that both these systems exhibit certain characteristics showing the presence of α-agostic bonds. Systems **C2EA**, **C2EB**, and **C2PG** were studied on the basis of local density approximation by Han et al.[11] who reported particularly small values of the Co−C−H angle (63.1°) and the Co···H distance (1.666 Å) in **C2EA**. Extremely small values of these parameters suggest the presence of a strong α-agostic bond that might be traced by a bond path. Already at this point, however, we mention that, in spite of the fact that values of some geometrical parameters suggest the presence of α-agostic bonds in systems **C2MA**, **C2EA**, **T2MA**, and **T2EA**, bond

DOI: 10.1021/acs.jpca.5b02041
J. Phys. Chem. A 2015, 119, 4993−5008

Table 1. Values of the Most Important Geometric Parameters Relating to Intramolecular Charge-Inverted Hydrogen Bonds in Systems Shown in Figure 1

functional	system	d_{SiH}	d_{SiH_i}	$d_{H\cdots Al}$	$d_{Si\cdots Al}$	α_{SiHAl}	system	d_{SiH}	d_{SiH_i}	$d_{H\cdots Al}$	$d_{Si\cdots Al}$	α_{SiHAl}
BP86	**0**	1.501; 1.500	1.504	3.290	2.467	45.0	**1**[a]	2 × 1.494	1.539	2.363	2.780	88.2
B3LYP		2 × 1.489	1.492	3.283	2.466	45.0		1.487[b]	2 × 1.488[b]	3.624[b]	3.251[b]	63.7[b]
B3PW91		2 × 1.492	1.495	3.279	2.461	45.0		2 × 1.487	1.518	2.567	2.865	85.0
PBE0		2 × 1.493	1.496	3.276	2.460	45.1		2 × 1.486	1.537	2.282	2.730	89.1
TPSSh		2 × 1.489	1.492	3.287	2.467	44.9		2 × 1.482	1.535	2.230	2.720	90.6
M06-L		2 × 1.485	1.488	3.269	2.452	44.9		2 × 1.476	1.537	2.123	2.652	91.5
M06		1.485	1.488; 1.487	3.29; 3.30	2.457	44.5; 43.9		2 × 1.479	1.512	2.520	2.823	85.4
BP86	**2s**	1.496; 1.495	1.539	2.103	3.073	114.2	**4sss**	1.497; 1.492	1.534	1.996	3.122	123.9
B3LYP		2 × 1.483	1.520	2.209	3.145	113.7		1.484; 1.480	1.515	2.033	3.204	128.5
B3PW91		1.487; 1.486	1.529	2.107	3.062	113.8		1.488; 1.483	1.524	1.994	3.106	123.4
PBE0		1.488; 1,487	1.532	2.082	3.037	113.5		1.490; 1.484	1.527	1.981	3.072	121.7
TPSSh		1.483; 1.482	1.528	2.048	3.027	114.9		1.485; 1.479	1.522	1.960	3.065	122.8
M06-L		2 × 1.477	1.519	2.067	3.033	114.7		1.479; 1.475	1.512	1.999	3.106	123.8
M06		1.480; 1.479	1.517	2.180	3.091	112.2		1.480; 1.478	1.512	2.055	3.152	123.4
BP86	**2d**	2 × 1.496	1.540	2.054	3.085	117.6	**4dss**	1.495; 1.492	1.538	1.931	3.013	120.2
B3LYP		2 × 1.483	1.523	2.102	3.113	117.4		1.482; 1.480	1.518	1.957	3.079	124.3
B3PW91		2 × 1.487	1.531	2.045	3.064	117.2		1.487; 1.482	1.525	1.990	3.178	128.9
PBE0		2 × 1.488	1.532	2.028	3.048	117.1		1.488; 1.484	1.530	1.921	2.976	118.7
TPSSh		2 × 1.484	1.529	1.999	3.039	118.4		1.483; 1.478	1.523	1.952	3.128	127.9
M06-L		2 × 1.478	1.520	2.009	3.043	118.5		1.477; 1.475	1.516	1.934	3.006	120.8
M06		2 × 1.480	1.519	2.075	3.079	117.0		1.479; 1.476	1.516	1.971	3.033	120.3
BP86	**3ss**	2 × 1.494	1.537	2.012	3.076	119.6	**4sds**	1.497; 1.492	1.528	1.983	3.351	145.0
B3LYP		2 × 1.482	1.519	2.064	3.138	121.6		1.484; 1.480	1.512	2.028	3.382	145.2
B3PW91		2 × 1.485	1.527	2.012	3.065	119.4		1.488; 1.483	1.517	1.987	3.340	144.4
PBE0		1.487; 1.486	1.529	1.998	3.041	118.5		1.489; 1.484	1.518	1.976	3.324	143.8
TPSSh		1.482; 1.481	1.524	1.977	3.035	119.6		1.484; 1.480	1.514	1.949	3.310	145.5
M06-L		1.477; 1.476	1.515	2.024	3.071	119.7		1.479; 1.475	1.505	1.978	3.335	146.1
M06		1.479; 1.478	1.515	2.081	3.114	119.2		1.479; 1.476	1.511	2.021	3.116	123.1
BP86	**3ds**	1.497; 1.493	1.544	1.968	3.152	127.2	**4ssd**	1.494; 1.493	1.532	1.963	3.034	120.0
B3LYP		1.484; 1.480	1.525	1.996	3.178	128.4		1.482; 1.481	1.514	1.990	3.091	123.3
B3PW91		1.488; 1.484	1.533	1.966	3.131	126.5		1.486; 1.484	1.522	1.957	3.020	119.9
PBE0		1.489; 1.485	1.535	1.956	3.111	125.6		1.487; 1.485	1.525	1.948	2.994	118.6
TPSSh		1.484; 1.480	1.531	1.935	3.106	127.0		1.483; 1.480	1.520	1.935	2.987	119.2
M06-L		1.480; 1.475	1.523	1.962	3.129	127.4		1.477; 1.476	1.511	1.966	3.018	119.8
M06		1.481; 1.476	1.522	2.012	3.156	126.0		1.479; 1.478	1.512	2.005	3.055	120.0
BP86	**3sd**	1.496; 1.492	1.531	1.993	3.137	125.2	**4dsd**	1.495; 1.491	1.540	1.939	2.960	116.1
B3LYP		1.483; 1.480	1.515	2.037	3.179	126.4		1.481; 1.479	1.520	1.964	3.037	120.8
B3PW91		1.487; 1.483	1.522	1.994	3.121	125.5		1.486; 1.482	1.530	1.940	2.952	116.0
PBE0		1.488; 1.484	1.524	1.987	3.100	123.5		1.488; 1.483	1.533	1.932	2.924	114.6
TPSSh		1.483; 1.479	1.519	1.960	3.093	125.0		1.483; 1.478	1.529	1.918	2.916	115.1
M06-L		1.478; 1.475	1.509	2.017	3.129	124.4		1.477; 1.474	1.518	1.957	2.945	115.3
M06		1.479; 1.477	1.509	2.090	3.183	123.6		1.478; 1.475	1.518	1.993	2.996	116.5

[a]Somewhat more stable form with two Si−H···Al contacts (no bond paths) has also been obtained by means of some functionals. [b]Full geometry optimization has led to the form with two Si−H···Al contacts (no bond paths).

paths have not been found in any of these systems. Similarly, our calculations have shown that neither the eclipsed form (in fact occurring to be a transition state and proclaimed earlier[28] as revealing some features indicating a presence of an α-agostic bond) nor the staggered conformer of $[Ti(Cl_2)Me]^+$ features a H···Ti bond path. These are the evidence that α-agostic bonds are never traced by a concomitant bond path (so far we do not know any case showing that this conclusion is not valid), and therefore, in fact, they should not be called bonds.[29,30] It should also be mentioned that in many instances the agostic carbon can successfully compete for a bond path to the metal atom.[30] However, as already underlined, our model systems possess agostic bonds that are "stable" with respect to the utilized set of exchange−correlation functionals.

RESULTS AND DISCUSSION

Geometrical Data. Values of the most important geometric parameters relating to intramolecular charge-inverted hydrogen bonds in systems shown in Figure 1 are gathered in Table 1. First, let us discuss the influence of the used exchange−correlation functional on values of chosen geometric parameters describing IMCIHB. It is clearly seen from Table 1 that the investigated functionals form the following order of Si−H bond lengths: M06-L, M06 < B3LYP, TPSSh < PBE0, B3PW91 < BP86. On the contrary, B3LYP and M06 give significantly longer H···Al distances than all the other functionals. This discrepancy, however, becomes smaller for larger systems. All other functionals give similar H···Al distances, those obtained by TPSSh being marginally smaller. If H···Al distances were to

DOI: 10.1021/acs.jpca.5b02041
J. Phys. Chem. A 2015, 119, 4993−5008

Table 2. Values of Some Chosen Geometric Parameters Characterizing Model Systems with H···M (M = Co, Ti) β-, γ-, and δ-Agostic Bonds Shown in Figure 2

system	functional	$d_{C_\alpha H}$	$d_{C_\alpha H_\alpha}$	$d_{H_\alpha \cdots M}$	$d_{C_\alpha \cdots M}$	$\alpha_{C_\alpha H_\alpha M}$	$\alpha_{MC_\alpha C_\beta}$	$\alpha_{C_\alpha C_\beta C_\gamma}$	$\alpha_{C_\beta C_\gamma C_\delta}$	$\alpha_{CC_\alpha H_\alpha}$
C1EB	BP86	2 × 1.104	1.267	1.609	2.148	95.9	74.5			112.8
	B3LYP	2 × 1.095	1.228	1.632	2.193	99.2	73.9			113.9
	B3PW91	2 × 1.097	1.238	1.612	2.156	97.5	74.0			113.7
	PBE0	1.101; 1.095	1.233	1.617	2.150	97.0	73.7			114.1
	TPSSh	2 × 1.096	1.253	1.599	2.163	97.9	74.6			112.1
	M06-L	2 × 1.095	1.204	1.661	2.141	95.4	75.3			114.2
	M06	1.107; 1.091	1.209	1.665	2.139	94.8	72.7			115.1
C1PG	BP86	1.113; 1.101	1.211	1.672	2.107	92.5	82.7	109.6		120.2
	B3LYP	1.099; 1.091	1.188	1.669	2.139	95.5	82.1	111.5		119.6
	B3PW91	1.101; 1.093	1.195	1.660	2.087	92.5	80.7	111.4		119.7
	PBE0	1.101; 1.093	1.195	1.658	2.069	91.5	79.4	112.2		119.3
	TPSSh	1.101; 1.093	1.201	1.655	2.069	93.1	80.1	111.6		119.4
	M06-L	1.101; 1.091	1.179	1.694	2.090	91.6	80.7	110.4		119.2
	M06	1.100; 1.094	1.183	1.679	2.064	90.6	79.0	112.0		119.0
C1BG	BP86	1.110	1.268	1.600	2.214	100.4	83.0	112.0	119.6	116.4
	B3LYP	1.097	1.242	1.597	2.222	102.2	82.5	113.2	118.9	116.1
	B3PW91	1.101	1.244	1.592	2.125	96.3	79.4	113.8	119.2	115.7
	PBE0	1.102	1.238	1.597	2.063	92.5	77.2	115.1	118.9	114.2
	TPSSh	1.100	1.249	1.592	2.144	97.3	79.4	113.8	119.0	115.8
	M06-L	1.103	1.215	1.635	2.104	94.0	78.9	113.1	118.7	114.6
	M06	1.098	1.219	1.638	1.988	86.9	75.0	118.1	116.5	109.6
C1bD	BP86	1.114; 1.107	1.181	1.723	2.207	97.2	114.0	122.4	112.9	112.0
	B3LYP	1.101, 1.095	1.164	1.725	2.242	100.0	114.0	123.2	113.3	111.6
	B3PW91	1.104; 1.100	1.166	1.727	2.181	95.9	113.5	122.5	112.8	111.8
	PBE0	1.105; 1.101	1.165	1.732	2.159	94.3	113.3	122.3	112.7	111.9
	TPSSh	1.103; 1.099	1.170	1.714	2.202	97.8	113.8	122.7	112.7	110.8
	M06-L	1.100; 1.099	1.148	1.787	2.215	95.6	114.6	122.7	112.8	111.4
	M06	1.102; 1.101	1.159	1.751	2.179	94.8	114.2	122.3	112.4	111.7
C2EB	BP86	1.098; 1.094	1.233	1.633	2.126	94.8	74.2			113.1
	B3LYP	1.088; 1.085	1.192	1.674	2.157	96.2	76.2			112.2
	B3PW91	1.089; 1.086	1.206	1.642	2.124	95.2	75.3			112.4
	PBE0	1.090; 1.087	1.205	1.640	2.117	94.9	75.2			112.5
	TPSSh	1.090; 1.086	1.214	1.636	2.127	95.4	75.0			112.3
	M06-L	1.088; 1.085	1.185	1.674	2.136	95.1	75.5			113.3
	M06	1.089; 1.087	1.190	1.667	2.132	95.1	75.7			113.0
C2PG	BP86	1.100; 1.095	1.152	1.769	2.421	110.2	96.0	106.9		115.0
	B3LYP	1.090; 1.087	1.128	1.853	2.501	111.7	97.4	108.3		114.0
	B3PW91	1.092; 1.088	1.136	1.792	2.425	109.8	96.3	107.3		114.8
	PBE0	1.092; 1.088	1.136	1.786	2.405	108.7	96.0	106.9		115.0
	TPSSh	1.093; 1.088	1.141	1.767	2.412	110.2	95.8	106.6		114.4
	M06-L	1.089; 1.087	1.127	1.834	2.450	109.3	96.1	107.5		114.3
	M06	1.091; 1.089	1.133	1.794	2.417	109.3	96.2	106.8		114.7
T1EB	BP86	2 × 1.097	1.155	2.035	2.401	93.5	84.4			114.4
	B3LYP	2 × 1.088	1.146	2.029	2.401	94.1	84.8			113.9
	B3PW91	2 × 1.089	1.147	2.022	2.384	93.5	84.6			114.3
	PBE0	2 × 1.089	1.148	2.014	2.374	93.2	84.4			114.4
	TPSSh	2 × 1.089	1.151	2.009	2.392	94.5	84.3			113.6
	M06-L	2 × 1.087	1.142	2.001	2.378	94.4	84.0			114.2
	M06	1.089; 1.088	1.143	2.020	2.363	92.4	83.8			114.6

suggest the strength of IMCIHBs, then B3LYP and M06 would lead to the weakest and TPSSh to the strongest IMCIHBs; however, it is not easy to reliably assess the strength of IMCIHBs as it would require a choice of a reference system with no IMCIHB. Any such choice would have been arbitrary in fact.[4] All exchange−correlation functionals lead to similar values of α_{SiHAl} angles; however, somewhat greater values of α_{SiHAl} can be seen in some cases if B3LYP is used. All these findings will later be confronted with those obtained for agostic systems.

To simplify the general characteristics of IMCIHB in the investigated model systems, we have chosen results obtained by means of the TPSSh functional. As already mentioned, this functional has recently been shown by Bühl and Kabrede[33] to give the best geometries of first row transition metal complexes if compared to experimental structures and will also be used to characterize investigated systems with agostic bonds. Moreover,

DOI: 10.1021/acs.jpca.5b02041
J. Phys. Chem. A 2015, 119, 4993−5008

Table 3. Values of Some Chosen Geometric Parameters Characterizing Model Systems with H···M (M = Co, Ti) α-Agostic Bonds Shown in Figure 2

system	functional	d_{C_aH}	$d_{C_aH_a}$	$d_{H_a\cdots M}$	$\alpha_{MC_aH_a}$	$\alpha_{C_aH_aM}$	$\alpha_{MC_a\beta}$	$\alpha_{H_aC_aH}$	α_{HC_aH}
C2MA	BP86	2 × 1.094	1.156	1.905	73.9	70.5			
	B3LYP	1.086; 1.085	1.117	2.150	86.7	62.1			
	B3PW91	1.088; 1.086	1.125	2.073	83.1	64.3			
	PBE0	1.088; 1.087	1.125	2.075	83.5	63.9			
	TPSSh	2 × 1.087	1.143	1.931	75.5	69.5			
	M06-L	2 × 1.085	1.141	1.900	73.9	70.9			
	M06	2 × 1.086	1.146	1.894	74.0	70.4			
C2EA	BP86	1.098	1.200	1.729	64.6	76.6	127.7		
	B3LYP	1.087	1.163	1.817	69.3	73.9	132.9		
	B3PW91	1.089	1.174	1.774	67.7	74.6	133.3		
	PBE0	1.090	1.174	1.775	68.0	74.2	133.1		
	TPSSh	1.090	1.183	1.748	66.1	75.7	133.0		
	M06-L	1.089	1.171	1.763	66.5	76.0	132.4		
	M06	1.090	1.177	1.756	66.7	75.3	132.6		
T2MA	BP86	2 × 1.099	1.103	2.553	101.1	53.8		109.4	109.6
	B3LYP	2 × 1.090	1.093	2.552	101.8	53.4		109.5	109.9
	B3PW91	2 × 1.091	1.095	2.534	101.3	53.7		109.4	109.9
	PBE0	2 × 1.091	1.096	2.527	101.2	53.6		109.4	109.9
	TPSSh	2 × 1.092	1.097	2.543	101.0	54.0		109.4	109.8
	M06-L	2 × 1.089	1.094	2.534	100.8	54.1		109.4	109.6
	M06	2 × 1.091	1.095	2.535	101.2	53.7		109.5	109.8
	exp[a]	**2 × 1.095**	**1.100**					**108.9**	**107.5**
T2EA	BP86	1.102	1.109	2.439	93.6	59.4	122.7	107.1	
	B3LYP	1.093	1.098	2.451	95.0	58.5	121.9	107.2	
	B3PW91	1.094	1.101	2.428	94.2	58.9	122.2	107.0	
	PBE0	1.094	1.101	2.424	94.4	58.7	121.5	107.0	
	TPSSh	1.095	1.102	2.436	94.0	59.1	121.8	107.3	
	M06-L	1.093	1.099	2.428	93.8	59.4	120.8	107.1	
	M06	1.094	1.101	2.426	94.1	59.0	121.4	107.1	
	exp[a]	**1.100**	**1.105**					**106.3**	

[a]Experimental values estimated by Robertson et al.[10] on the basis of infrared spectra.

it will soon be shown that, indeed, TPSSh (and BP86) yields values of geometrical parameters being the closest to the experimental results.

First of all it is seen that the interacting Si−H bond (Si−H_i in Table 1) is significantly longer than the other two Si−H bonds; thus, as already reported,[3] formation of IMCIHB leads to the elongation of the interacting Si−H bond. If we take into account those IMCIHBs that are traced by the presence of the H···Al bond path (i.e., excluding H···Al contacts in **0** and **1**), then the length of IMCIHB is in the range 1.92−2.05 Å, being systematically no shorter than 2.00 Å in molecules **2s** and **2d** possessing a five-membered quasi-ring. If one goes to **1** possessing a four-membered quasi-ring, then the H···Al distance significantly increases to 2.23 Å—high enough to not create a bond path. This shows that the strain in a molecule opposes the IMCIHB formation.[3] Interestingly, although not traced by the presence of $BP_{H\cdots Al}$, greater values of d_{SiH_i} in comparison with d_{SiH} also indicate H···Al interaction in **0** and, in particular, in **1**. Therefore, the geometric trace of an interatomic interaction does not necessarily go hand in hand with topological proof in the form of the presence of a bond path. This important conclusion has already been reported earlier.[28]

Values of some chosen geometrical parameters characterizing model systems with H···M (M = Ti, Co) β-, γ-, and δ-agostic bonds are shown in Table 2 and those with α-agostic bonds in Table 3. Similarly, as it was in the case of systems with IMCIHB, BP86 clearly gives longer C−H bonds (both C_a−H and C_a−H_a) and M06 and, in particular, M06-L and B3LYP tend to give them the shortest among all exchange−correlation functionals used in this study. The difference between the greatest and the lowest values of d_{C_aH} and $d_{C_aH_a}$ can be significant; e.g., in the case of **C1EB** it amounts to 0.009 and 0.063 Å, respectively, if BP86 and M06-L results are compared. Much more complex dependence on the exchange−correlation functional has been found for $d_{H_a\cdots M}$. Namely, the longest H_a···M distances have been obtained by means of not only M06-L or M06 functionals but also B3LYP (in **C2EB**, **C2PG**, **C2MA**, **C2EA**, and **T2EA**) and BP86 (**T1EB**, **T2MA**) can lead to greatest values. On the contrary, similarly as for IMCIHBs, TPSSh tends to lead to the shortest H_a···M distances in the **C1** set, whereas for **C2EA**, **C2EB**, and **C2PG** BP86 may compete. Discussion on the C_a···M distances obtained by means of diverse exchange−correlation functionals may indicate a preference for the creation of a bond path to a carbon instead of to a hydrogen. On the basis of a vanadium complex, Tognetti and Joubert have shown (see Figure 6 in ref 32) that DFT-based calculations using PBE0 functional have led to the C···V bond path, whereas those with TPSS to H···V instead. As can be seen from Table 2, for the largest systems **C1bD**, **C2EB**, and **C2PG** PBE0 leads to somewhat shorter C_a···M distances than all the other functionals. However, in some cases M06 may lead to even shorter C_a···M distances, as evidenced in particular by

DOI: 10.1021/acs.jpca.5b02041
J. Phys. Chem. A 2015, 119, 4993−5008

Table 4. Values of Some Chosen QTAIM Parameters Characterizing Model Systems with IMCIHB Shown in Figure 1

system	functional	ρ_b	$\nabla^2\rho_b$	H_b	λ_1	λ_2	λ_3	ε	d_{br}	ρ_r	$\Delta\rho_{br}$
2s	BP86	0.024	0.037	−0.005	−0.018	−0.007	0.062	1.4	0.69	0.022	0.002
	B3LYP	0.020	0.026	−0.003	−0.015	−0.003	0.044	4.6	0.32	0.019	0.000
	B3PW91	0.023	0.038	−0.004	−0.017	−0.003	0.058	4.7	0.59	0.022	0.001
	PBE0	0.024	0.045	−0.004	−0.018	−0.005	0.068	2.6	0.63	0.023	0.001
	TPSSh	0.025	0.056	−0.004	−0.020	−0.009	0.085	1.1	0.73	0.023	0.002
	M06-L	0.023	0.053	−0.003	−0.018	−0.006	0.077	2.0	0.67	0.022	0.001
	M06	*a*	*a*	*a*	*a*	*a*	*a*	*a*	*a*	*a*	*a*
2d	BP86	0.025	0.046	−0.004	−0.020	−0.013	0.078	0.6	0.80	0.021	0.004
	B3LYP	0.022	0.041	−0.004	−0.017	−0.008	0.066	1.2	0.72	0.020	0.002
	B3PW91	0.025	0.054	−0.004	−0.020	−0.012	0.085	0.7	0.77	0.022	0.003
	PBE0	0.025	0.058	−0.004	−0.021	−0.013	0.092	0.6	0.79	0.022	0.003
	TPSSh	0.026	0.068	−0.004	−0.023	−0.016	0.106	0.4	0.83	0.022	0.004
	M06-L	0.025	0.068	−0.003	−0.021	−0.014	0.103	0.5	0.82	0.021	0.004
	M06	0.023	0.045	−0.004	−0.018	−0.007	0.071	1.4	0.71	0.021	0.002
3ss	BP86	0.026	0.056	−0.004	−0.021	−0.016	0.093	0.3	1.24	0.015	0.011
	B3LYP	0.023	0.046	−0.004	−0.017	−0.012	0.075	0.5	1.18	0.014	0.009
	B3PW91	0.026	0.062	−0.004	−0.020	−0.015	0.097	0.3	1.22	0.016	0.010
	PBE0	0.026	0.067	−0.004	−0.021	−0.016	0.104	0.3	1.22	0.016	0.010
	TPSSh	0.027	0.075	−0.003	−0.023	−0.018	0.116	0.3	1.24	0.016	0.011
	M06-L	0.024	0.065	−0.002	−0.018	−0.013	0.097	0.4	1.20	0.015	0.009
	M06	0.022	0.045	−0.004	−0.016	−0.009	0.070	0.9	1.11	0.015	0.007
3ds	BP86	0.029	0.060	−0.005	−0.025	−0.021	0.106	0.2	1.24	0.014	0.014
	B3LYP	0.026	0.056	−0.004	−0.022	−0.018	0.096	0.3	1.21	0.013	0.013
	B3PW91	0.028	0.068	−0.004	−0.024	−0.020	0.113	0.2	1.22	0.015	0.013
	PBE0	0.028	0.072	−0.004	−0.025	−0.021	0.118	0.2	1.22	0.015	0.013
	TPSSh	0.029	0.082	−0.004	−0.027	−0.023	0.132	0.1	1.24	0.015	0.014
	M06-L	0.027	0.076	−0.003	−0.024	−0.020	0.121	0.2	1.22	0.014	0.013
	M06	0.025	0.056	−0.004	−0.021	−0.016	0.093	0.3	1.17	0.014	0.011
3sd	BP86	0.027	0.059	−0.004	−0.021	−0.018	0.098	0.1	1.25	0.014	0.012
	B3LYP	0.023	0.051	−0.003	−0.018	−0.014	0.083	0.3	1.20	0.013	0.010
	B3PW91	0.026	0.065	−0.003	−0.020	−0.017	0.102	0.1	1.23	0.014	0.011
	PBE0	0.026	0.068	−0.004	−0.020	−0.018	0.106	0.1	1.22	0.015	0.011
	TPSSh	0.027	0.078	−0.003	−0.022	−0.020	0.121	0.1	1.25	0.015	0.012
	M06-L	0.023	0.067	−0.002	−0.017	−0.015	0.099	0.2	1.20	0.014	0.010
	M06	0.021	0.045	−0.003	−0.014	−0.009	0.069	0.5	1.11	0.014	0.007
4sss	BP86	0.027	0.057	−0.004	−0.021	−0.018	0.096	0.2	1.74	0.010	0.017
	B3LYP	0.024	0.053	−0.003	−0.018	−0.015	0.085	0.2	1.69	0.009	0.015
	B3PW91	0.026	0.064	−0.004	−0.020	−0.017	0.102	0.2	1.73	0.010	0.016
	PBE0	0.027	0.069	−0.004	−0.021	−0.018	0.108	0.2	1.74	0.011	0.016
	TPSSh	0.027	0.078	−0.003	−0.023	−0.020	0.121	0.2	1.76	0.011	0.017
	M06-L	0.024	0.070	−0.002	−0.019	−0.016	0.106	0.2	1.76	0.010	0.014
	M06	0.022	0.051	−0.003	−0.017	−0.012	0.079	0.4	1.69	0.010	0.012
4dss	BP86	0.030	0.077	−0.005	−0.027	−0.024	0.127	0.1	1.82	0.011	0.019
	B3LYP	0.028	0.073	−0.004	−0.024	−0.021	0.118	0.1	1.75	0.010	0.018
	B3PW91	0.026	0.064	−0.004	−0.020	−0.018	0.102	0.1	1.37	0.009	0.017
	PBE0	0.030	0.088	−0.004	−0.027	−0.024	0.139	0.1	1.81	0.012	0.018
	TPSSh	0.027	0.078	−0.003	−0.023	−0.021	0.122	0.1	1.36	0.009	0.018
	M06-L	0.028	0.091	−0.002	−0.025	−0.022	0.138	0.1	1.79	0.011	0.017
	M06	0.027	0.072	−0.003	−0.023	−0.019	0.114	0.2	1.75	0.011	0.016
4sds	BP86	0.026	0.054	−0.004	−0.021	−0.020	0.095	0.0	1.45	0.008	0.018
	B3LYP	0.023	0.050	−0.003	−0.017	−0.016	0.083	0.0	1.43	0.007	0.016
	B3PW91	0.025	0.060	−0.003	−0.019	−0.018	0.097	0.0	1.44	0.008	0.017
	PBE0	0.025	0.063	−0.003	−0.020	−0.019	0.101	0.0	1.43	0.008	0.017
	TPSSh	0.026	0.074	−0.003	−0.022	−0.021	0.118	0.0	1.43	0.008	0.018
	M06-L	0.024	0.070	−0.002	−0.019	−0.018	0.108	0.0	1.44	0.008	0.016
	M06	0.024	0.059	−0.003	−0.018	−0.015	0.092	0.2	1.62	0.010	0.014
4ssd	BP86	0.029	0.068	−0.004	−0.024	−0.021	0.113	0.1	1.63	0.011	0.018
	B3LYP	0.026	0.065	−0.004	−0.020	−0.020	0.105	0.0	1.56	0.009	0.016
	B3PW91	0.028	0.076	−0.004	−0.023	−0.021	0.121	0.1	1.62	0.011	0.017
	PBE0	0.029	0.080	−0.004	−0.024	−0.022	0.127	0.1	1.63	0.012	0.017
	TPSSh	0.029	0.088	−0.003	−0.026	−0.024	0.137	0.1	1.67	0.012	0.017

DOI: 10.1021/acs.jpca.5b02041
J. Phys. Chem. A 2015, 119, 4993−5008

Table 4. continued

system	functional	ρ_b	$\nabla^2\rho_b$	H_b	λ_1	λ_2	λ_3	ε	d_{br}	ρ_r	$\Delta\rho_{br}$
	M06-L	0.026	0.083	−0.002	−0.022	−0.020	0.124	0.1	1.64	0.011	0.015
	M06	0.025	0.063	−0.003	−0.019	−0.017	0.100	0.1	1.55	0.011	0.014
4dsd	BP86	0.030	0.075	−0.005	−0.027	−0.023	0.126	0.2	1.72	0.013	0.018
	B3LYP	0.028	0.070	−0.004	−0.023	−0.022	0.115	0.1	1.62	0.011	0.016
	B3PW91	0.030	0.083	−0.004	−0.026	−0.023	0.132	0.2	1.68	0.013	0.016
	PBE0	0.030	0.087	−0.004	−0.027	−0.024	0.138	0.2	1.69	0.014	0.016
	TPSSh	0.031	0.097	−0.003	−0.029	−0.025	0.151	0.2	1.71	0.014	0.016
	M06-L	0.027	0.087	−0.002	−0.024	−0.021	0.132	0.2	1.66	0.013	0.014
	M06	0.026	0.069	−0.004	−0.022	−0.018	0.109	0.2	1.60	0.013	0.013

[a] $BP_{H\cdots C}$ instead of $BP_{H\cdots Al}$ has been obtained; see Figure 4.

C1BG (1.988 and 2.063 Å for M06 and PBE0, respectively). It will soon be shown that in this system, indeed, the M06 functional leads to the M···C_γ bond path instead of to the M···H_γ one. Considering bond angles one can see that differences between their values can be sizable, particularly in system **C1BG**, i.e., $[Co(Cl_2)^nBu]^{2+}$. This likely results from the floppy position of the ethyl group with respect to the other part of the molecule. For example, values of $\alpha_{C_aH_aM}$ obtained by means of B3LYP and M06 are 102.2° and 86.9°, respectively, yielding a difference of 15.3°. A similarly large difference (12.8°) has been obtained for $\alpha_{MC_aH_a}$ in **C2MA** (73.9° from BP86 and M06-L and 86.7° from B3LYP; Table 3), showing that the B3LYP functional weakly favors α-agostic geometry in this complex. It is worth mentioning that the considerable preference of systems **C2EA**, **C2EB**, and **C2PG** to accept an agostic geometry found earlier by Han et al.[11] is significantly weakened if our set of exchange−correlation functionals is used as indicated by smaller values of $d_{C_aH_a}$ and greater values of $d_{H_a\cdots M}$, $d_{C_a\cdots M}$, and relevant bond angles indicating a less strained quasi-ring. This likely results from the local density approximation they used.

The above analysis gives the opportunity for finding common conclusions for both IMCIHBs and ABs. Namely, among all investigated exchange−correlation functionals BP86 gives the longest either Si−H and Si−H_i or C_a−H and C_a−H_a bonds, whereas M06-L and M06 tend to give them the shortest. Furthermore, M06 and B3LYP give the longest either H···Al or H_a···M distances among all investigated exchange−correlation functionals. At the same time M06 tends to give the shortest values of $d_{C_a\cdots M}$ in **C1EB**, **C1PG**, **C1BG**, and **T1EB** (PBE0 in **C1bD**, **C2EB**, and **C2PG**) showing some preference to the M···C_a bond path over the M···H_a one.

To test the performance of exchange−correlation functionals investigated in this study, we have compared computed values of some geometrical parameters with experimental values obtained by Robertson et al.[10] for **T2MA** and **T2EA** complexes. These values are printed in Table 3 in boldface. In accordance with the conclusion of Bühl and Kabrede,[33] TPSSh indeed gives the best values of geometrical parameters in comparison to experimental data. It is seen from Table 3 that also BP86 performs well, again in line with the previous work.[33] As a consequence, to give a brief description of an agostic bond and then to compare it with an intramolecular charge-inverted hydrogen bond we shall only take into account results obtained by means of the TPSSh functional.

As expected and similarly as in the case of IMCIHB, formation of an agostic bond leads to a significant elongation of the C−H bond participating in AB. The H_a···Co distance is in the range from 1.592 Å (molecule **C1BG**) to 1.931 Å (molecule **C2MA**), whereas H_a···Ti is much greater (from 2.009 Å in **T1EB** to 2.436 and 2.543 Å in **T2EA** and **T2MA**, respectively). Taking into account cobalt complexes with formal +1 charge (the middle row in Figure 2), it becomes clear that the H_a···M distance is the shortest in the case of the β-agostic bond. The H_a···Co distance in **C2EB** is 1.636 Å only, whereas it amounts to 1.748 Å (**C2EA**) to 1.931 Å (**C2MA**) in α-agostic systems and 1.767 Å in **C2PG** possessing an agostic bond of γ-type. This conclusion is in line with earlier reports.[14,15] On increasing the formal charge on the cobalt atom from +1 to +2 (the upper row in Figure 2), $d_{H_a\cdots Co}$ decreases, e.g., from 1.636 Å in **C2EB** to 1.599 Å in **C1EB** or from 1.767 Å in **C2PG** to 1.655 Å in **C1PG**. It is known, however, that in general the dependence of the H_a···M distance on the type of a transition metal, its formal charge, and the type of an agostic bond is much more complex.[12,14,15] Although the range of H···Al distances for systems with IMCIHB (1.92−2.05 Å) is included in the range of $d_{H_a\cdots M}$ (M = Ti, Co) for agostic bonds (1.592−2.543 Å), it is outside and shifted upward with respect to the latter if α-agostic bonds, i.e., interactions not traced by a H···M bond path, are excluded (1.592−1.767 Å). It shows that IMCIHBs are longer than ABs; however, we have not considered neutral complexes possessing β-, γ-, or δ-agostic bonds that likely would widen the range of $d_{H_a\cdots M}$ toward somewhat greater values.

QTAIM-Based Analysis. In our earlier article[1] on the comparison of various interactions involving the $X^{\delta+}$−$H^{\delta-}$ unit, some preliminary studies have already been made in the direction of comparison intramolecular charge-inverted hydrogen bonds with agostic bonds. As already mentioned in the Introduction, these comparative studies, however, require their continuation as different exchange−correlation functionals and basis sets were used in cited references referring to QTAIM results for agostic bonds.[27−30] Moreover, it has been shown that both a molecular graph[32] and values of some QTAIM parameters[31,32] may depend on the choice of the functional. Therefore, the fundamental importance in this article is to study the influence of the exchange−correlation functional on values of some chosen QTAIM parameters. Values of these QTAIM parameters are collected in Tables 4 and 5 for systems with IMCIHBs and ABs, respectively.

Influence of Exchange−Correlation Functional on Values of QTAIM Parameters. Analyzing the data in Tables 4 and 5, it is concluded that the influence of the exchange−correlation functional on the value of the electron density (ρ_b) computed at either $BCP_{H\cdots Al}$ or $BCP_{H\cdots M}$ is very modest; nevertheless B3LYP, M06, and M06-L (for AB) yield somewhat lower

DOI: 10.1021/acs.jpca.5b02041
J. Phys. Chem. A 2015, 119, 4993−5008

Table 5. Values of Some Chosen QTAIM Parameters Characterizing Model Systems with Agostic Bonds Shown in Figure 2

system	functional	ρ_b	$\nabla^2\rho_b$	H_b	λ_1	λ_2	λ_3	ε	d_{br}	ρ_r	$\Delta\rho_{br}$
C1EB	BP86	0.101	0.160	−0.046	−0.151	−0.112	0.423	0.4	0.65	0.080	0.021
	B3LYP	0.093	0.185	−0.038	−0.131	−0.102	0.419	0.3	0.67	0.072	0.021
	B3PW91	0.099	0.172	−0.044	−0.144	−0.108	0.424	0.3	0.65	0.079	0.020
	PBE0	0.098	0.172	−0.043	−0.141	−0.104	0.417	0.4	0.64	0.080	0.019
	TPSSh	0.102	0.176	−0.046	−0.149	−0.117	0.443	0.3	0.65	0.079	0.023
	M06-L	0.089	0.229	−0.029	−0.116	−0.066	0.411	0.8	0.48	0.081	0.008
	M06	0.089	0.207	−0.031	−0.119	−0.064	0.389	0.9	0.57	0.080	0.009
C1PG	BP86	0.090	0.211	−0.031	−0.123	−0.059	0.394	1.1	1.07	0.057	0.033
	B3LYP	0.087	0.243	−0.029	−0.113	−0.059	0.415	0.9	1.07	0.051	0.036
	B3PW91	0.093	0.240	−0.033	−0.121	−0.054	0.415	1.2	1.05	0.059	0.034
	PBE0	0.094	0.249	−0.033	−0.120	−0.048	0.417	1.5	1.05	0.061	0.033
	TPSSh	0.093	0.243	−0.032	−0.121	−0.064	0.428	0.9	1.06	0.060	0.032
	M06-L	0.086	0.262	−0.025	−0.106	−0.027	0.395	3.0	0.95	0.062	0.024
	M06	0.090	0.265	−0.027	−0.109	−0.019	0.394	4.6	1.02	0.058	0.031
C1BG	BP86	0.102	0.152	−0.047	−0.160	−0.124	0.436	0.3	1.06	0.055	0.048
	B3LYP	0.101	0.189	−0.045	−0.153	−0.117	0.459	0.3	1.06	0.051	0.050
	B3PW91	0.106	0.186	−0.049	−0.160	−0.112	0.457	0.4	1.09	0.061	0.045
	PBE0	0.108	0.203	−0.049	−0.157	−0.096	0.456	0.6	1.11	0.066	0.042
	TPSSh	0.105	0.193	−0.048	−0.157	−0.117	0.468	0.3	1.08	0.061	0.044
	M06-L	0.097	0.231	−0.036	−0.137	−0.078	0.446	0.8	1.04	0.065	0.032
	M06	*a*	*a*	*a*	*a*	*a*	*a*	*a*	*a*	*a*	*a*
C1bD	BP86	0.079	0.191	−0.024	−0.109	−0.063	0.363	0.7	1.17	0.027	0.051
	B3LYP	0.076	0.200	−0.022	−0.103	−0.068	0.371	0.5	1.14	0.025	0.051
	B3PW91	0.080	0.203	−0.024	−0.106	−0.058	0.367	0.9	1.13	0.028	0.052
	PBE0	0.081	0.204	−0.025	−0.105	−0.051	0.361	1.1	1.12	0.029	0.052
	TPSSh	0.079	0.209	−0.024	−0.108	−0.067	0.384	0.6	1.15	0.028	0.052
	M06-L	0.069	0.210	−0.016	−0.085	−0.044	0.338	0.9	1.12	0.026	0.043
	M06	0.076	0.204	−0.021	−0.095	−0.042	0.341	1.3	1.10	0.028	0.048
C2EB	BP86	0.089	0.257	−0.033	−0.117	−0.076	0.450	0.5	0.57	0.077	0.012
	B3LYP	0.079	0.284	−0.023	−0.091	−0.056	0.430	0.6	0.47	0.072	0.007
	B3PW91	0.086	0.285	−0.030	−0.105	−0.065	0.455	0.6	0.50	0.078	0.008
	PBE0	0.087	0.290	−0.030	−0.104	−0.063	0.458	0.6	0.48	0.079	0.008
	TPSSh	0.087	0.291	−0.030	−0.107	−0.069	0.467	0.6	0.52	0.077	0.010
	M06-L	0.078	0.315	−0.020	−0.089	−0.042	0.446	1.1	0.39	0.075	0.003
	M06	0.081	0.292	−0.024	−0.094	−0.048	0.434	0.9	0.41	0.077	0.004
C2PG	BP86	0.057	0.202	−0.013	−0.065	−0.055	0.322	0.2	0.92	0.036	0.022
	B3LYP	0.044	0.179	−0.007	−0.047	−0.036	0.261	0.3	0.83	0.031	0.013
	B3PW91	0.053	0.207	−0.010	−0.057	−0.046	0.310	0.2	0.87	0.036	0.017
	PBE0	0.054	0.213	−0.011	−0.058	−0.047	0.318	0.2	0.87	0.037	0.017
	TPSSh	0.056	0.220	−0.012	−0.062	−0.052	0.333	0.2	0.90	0.037	0.020
	M06-L	0.046	0.202	−0.006	−0.047	−0.037	0.286	0.2	0.85	0.033	0.013
	M06	0.052	0.213	−0.010	−0.055	−0.044	0.311	0.3	0.87	0.037	0.016
T1EB	BP86	0.046	0.144	−0.003	−0.060	−0.025	0.229	1.4	0.21	0.045	0.001
	B3LYP	0.046	0.145	−0.003	−0.061	−0.031	0.237	1.0	0.24	0.044	0.001
	B3PW91	0.047	0.152	−0.004	−0.064	−0.028	0.243	1.3	0.21	0.047	0.001
	PBE0	0.049	0.155	−0.004	−0.066	−0.028	0.249	1.3	0.21	0.048	0.001
	TPSSh	0.048	0.149	−0.004	−0.066	−0.036	0.251	0.8	0.27	0.046	0.002
	M06-L	0.049	0.162	−0.003	−0.069	−0.035	0.266	0.9	0.26	0.047	0.002
	M06	0.048	0.164	−0.004	−0.064	−0.016	0.244	3.1	0.12	0.048	0.000

[a] $BP_{Co\cdots C_\gamma}$ instead of $BP_{Co\cdots H_\gamma}$ has been obtained.

values. As it will soon be shown, this results from more diffuse distribution of the charge density around BCP and is in line with greater H···Al and H···M (M = Ti, Co) distances obtained by means of these exchange−correlation functionals. On the contrary, TPSSh and BP86 (as well as PBE0 and B3PW91 in the case of AB) tend to somewhat greater values of ρ_b. Differences in computed values are more pronounced in the case of Laplacians ($\nabla^2\rho_b$). Namely, in the case of systems with IMCIHBs one can notice that TPSSh gives the greatest values, whereas M06 and B3LYP give them the lowest. In the case of agostic bonds, M06-L and M06 lead to the greatest values of $\nabla^2\rho_b$, whereas BP86 leads to the lowest. The used exchange−correlation functional does not have a great influence on the value of the electronic total energy density (H_b); however, for ABs, values somewhat closer to zero can be noticed if M06-L and M06 are employed. Importantly, all exchange−correlation functionals indicate the negative value of H_b. On the contrary, exchange−correlation functionals have a more noticeable effect

DOI: 10.1021/acs.jpca.5b02041
J. Phys. Chem. A 2015, 119, 4993−5008

on all curvatures calculated at BCPs (λ_i, i = 1, 2, 3), λ_3 (IMCIHB) or λ_2 and λ_3 (AB) in particular. They are larger if TPSSh is used; however, in the case of systems with an agostic bond, also BP86 has a tendency to yield more negative values of λ_1 and λ_2. On the contrary, M06 (and M06-L for AB) leads to the lowest values of all curvatures. This means that TPSSh leads to the most compact and M06 (and M06-L in AB) to the most flat distribution of the electron density in the closest vicinity of BCP. As a result of the described influence of exchange−correlation functionals on individual curvatures of the electron density distribution, the bond ellipticities (ε) computed at either $BCP_{H\cdots Al}$ or $BCP_{H\cdots M}$ are the greatest if M06 is used. This is particularly noticeable in systems with AB, where also M06-L and, in a lesser extent, PBE0 may lead to higher values of ε. On the contrary, due to a much more compact distribution of the electron density (in all directions of the local coordinate system; see large λ_i values) TPSSh yields the lowest bond ellipticities—again the result particularly evident in systems with agostic bonds. Importantly, one obtains much greater diversity of ε values for agostic bonds than for IMCIHBs. System **2s** deserves special attention, because some conspicuous deviations are seen if B3LYP and B3PW91 are utilized. Namely, both these functionals yield unexpectedly great values of ε (4.6 and 4.7, respectively). It should be noted that, when utilized to **2s**, M06 leads to the H···C bond path instead of to the H···Al one. Because the presence of IMCIHB in **2s** is evident (e.g., by the close H···Al distance and the significant elongation of the SiH_i bond), this result undermines the use of the M06 functional for QTAIM calculations, at least for IMCIHBs.

After analyzing Tables 4 and 5, one can summarize that in general the exchange−correlation functional has a negligible influence on values of the electron density and the electronic total energy density computed at either $BCP_{H\cdots Al}$ or $BCP_{H\cdots M}$. Much larger deviations are obtained in the case of $\nabla^2\rho_b$ and λ_3 (also λ_2 in ABs). Importantly for the future discussion, the positive sign of $\nabla^2\rho_b$ and the negative sign of H_b are preserved within the investigated set of exchange−correlation functionals.

Due to the quasi-closed structure of investigated molecules, all of them (but **0**, **1**, and systems with α-agostic bond) possess a ring critical point. The distance between BCP and RCP (d_{br}) as well as both the value of the electron density at this ring critical point (ρ_r) and the difference in electron densities computed at BCP and RCP ($\Delta\rho_{br}$) are also shown in Tables 4 and 5 for systems with IMCIHBs and ABs, respectively. The influence of exchange−correlation functionals on d_{br} seems to be more irregular and some clear deviations can easily be noticed. For example, particularly low values of d_{br} have been obtained in **T1EB** (0.12 Å, M06), **2s** (0.32 Å, B3LYP), and **4dss** (1.37 and 1.36 Å, B3PW91 and TPSSh, respectively). Nevertheless, one can notice a propensity of M06 to leading to somewhat lower values of d_{br} (in the case of IMCIHB also B3LYP and in the case of AB also M06-L tend to give lower d_{br}). This reflects somewhat lesser stability of some investigated systems if M06 is used.

More uniform influence of utilized functionals can be noticed in the case of ρ_r, i.e., the value of the electron density computed at RCP. This time both IMCIHBs and ABs feature the lowest values of ρ_r if computed by means of the DFT/B3LYP method. On the contrary, M06 (in some cases also M06-L in systems with AB) leads to the lowest values of $\Delta\rho_{br}$ among all investigated functionals. As already mentioned, this results from a flat distribution of electron density in the BCP-RCP direction as supported by the lowest values of $|\lambda_2|$ obtained by means of M06.

Comparative Study of Intramolecular Charge-Inverted Hydrogen Bonds and Agostic Bonds. As it was shown by Tognetti and Joubert,[32] the PBE0 functional belongs to the best performing for values of QTAIM parameters. Unfortunately, these authors did not consider either Minnesota M06-L and M06 functionals or the hybrid variant of TPSS, which, as already mentioned, was claimed by Bühl and Kabrede[33] and also confirmed in this study, to yield the best geometries for complexes with the first row transition metals if compared with experimental data. On the contrary, as Tognetti and Joubert concluded, the DFT functional providing excellent molecular geometries does not necessary yield the best values of local QTAIM parameters and vice versa.[32] Nevertheless, because at present we are going to perform comparative study of IMCIHBs and ABs that will be based on QTAIM computations, our choice of the exchange−correlation functional is henceforth PBE0. This functional was also used by Tognetti et al.[30] in their comprehensive study on agostic bond. It should be stressed, however, that in fact any other functional would lead to the same qualitative conclusions. We recall, however, that the M06 exchange−correlation functional wrongly led to the H···C bond path instead of to the H···Al one in system **2s**.

On the basis of data in Tables 4 and 5, one can conclude that values of the electron density computed at the bond critical point of the H···Al IMCIHB are fairly constant, being in the narrow range 0.024−0.030 au. They are much lower than electron density values computed at BCPs of investigated agostic bonds. The appropriate range for molecules with Co is 0.054−0.108 au, whereas ρ_b amounts to 0.049 au only for $C_2H_5TiCl_2^+$ (**T1EB**). Similarly, values of $\nabla^2\rho_b$ (0.045−0.088 au) computed at BCPs of IMCIHBs are lower than those computed at BCPs of agostic bonds (0.155−0.290 au). In spite of the fact that our ranges of ρ_b and $\nabla^2\rho_b$ computed for IMCIHBs are below those for agostic bonds, they both are contained in ranges of ρ_b and $\nabla^2\rho_b$ (0.01−0.13 au and 0.03−0.25 au, respectively) reported recently by Tognetti et al.[30] for a set of 23 complexes. This, however, may result from the fact that some δ-agostic bonds investigated by Tognetti et al. featured particularly low values of ρ_b and $\nabla^2\rho_b$; in our case the δ-agostic bond in molecule **C1bD** features relatively high values of ρ_b and $\nabla^2\rho_b$ due to the formal 2+ charge on the cobalt atom. Also, the particularly great value of $\nabla^2\rho_b$ found in **C2EB** (0.290 au) further extends the range reported earlier by Tognetti et al.[30] upward.

Importantly, both IMCIHBs and ABs are characterized by positive values of $\nabla^2\rho_b$ and negative values of H_b; thus, as a consequence, in spite of the fact that the latter are widely characterized as closed-shell interactions,[27,28,30] similarly as IMCIHBs, they also possess some covalent character. Because the value of H_b may in general strongly depend on the charge of interacting atoms, its sign cannot provide a good distinction between charge-inverted hydrogen bonds and agostic bonds.

It is often reported that agostic bonds are characterized by large values of $H_a\cdots M$ bond ellipticities.[27,28,30] Our calculations show, however, that ellipticities (ε) of agostic bonds in investigated group of model systems are rather low, being in the range 0.2−1.5. Moreover, small values of ε have also been obtained (0.0−0.6) for all, but **2s** (2.6), systems with IMCIHB. Let us recall, however, that the use of the M06 functional has led to significantly higher values of bond ellipticities,

DOI: 10.1021/acs.jpca.5b02041
J. Phys. Chem. A 2015, 119, 4993−5008

Table 6. Curvature of H···Al and H···M (M = Co, Ti) Bond Paths Tracing Intramolecular Charge-Inverted Hydrogen Bonds and Agostic Bonds, Respectively

functional	system	$l_{H\cdots BCP}$	$l_{BCP\cdots Al}$	Δ_{ld}	$\%_{HM}$	$\Delta\%_{HM}$	system	$l_{H_s\cdots BCP}$	$l_{BCP\cdots M}$	Δ_{ld}	$\%_{HM}$	$\Delta\%_{HM}$
BP86	**2s**	1.137	1.013	0.048	48	1.5	**C1EB**	0.634	0.991	0.017	62	0.4
B3LYP		1.209	1.487	0.488	55	8.4		0.665	0.991	0.025	61	0.4
B3PW91		1.163	1.025	0.081	48	2.9		0.648	0.989	0.026	61	0.5
PBE0		1.147	0.998	0.063	48	2.1		0.656	0.991	0.031	61	0.6
TPSSh		1.117	0.970	0.040	47	1.2		0.635	0.983	0.019	61	0.3
M06-L		1.135	0.985	0.054	48	1.8		0.722	0.984	0.045	59	1.1
M06		*a*	*a*	*a*	*a*	*a*		0.725	0.999	0.059	60	1.4
BP86	**2d**	1.096	0.982	0.025	48	0.7	**C1PG**	0.738	0.999	0.065	59	1.4
B3LYP		1.132	1.007	0.038	48	1.2		0.751	0.986	0.068	58	1.3
B3PW91		1.102	0.970	0.028	47	0.8		0.762	0.983	0.085	59	1.8
PBE0		1.093	0.961	0.027	47	0.7		0.781	0.978	0.102	58	2.2
TPSSh		1.074	0.946	0.022	47	0.6		0.739	0.981	0.066	59	1.4
M06-L		1.081	0.951	0.024	47	0.6		0.837	0.984	0.127	58	3.0
M06		1.125	0.998	0.048	48	1.6		0.872	0.978	0.171	58	4.2
BP86	**3ss**	1.069	0.962	0.020	48	0.4	**C1BG**	0.625	0.989	0.014	62	0.3
B3LYP		1.101	0.989	0.027	48	0.7		0.644	0.973	0.021	61	0.4
B3PW91		1.079	0.956	0.023	48	0.5		0.648	0.974	0.030	61	0.7
PBE0		1.073	0.949	0.024	47	0.5		0.672	0.972	0.047	60	1.1
TPSSh		1.059	0.938	0.021	47	0.4		0.644	0.971	0.023	61	0.5
M06-L		1.086	0.959	0.023	47	0.5		0.702	0.979	0.047	59	1.0
M06		1.120	0.999	0.039	48	1.2		*b*	0.988	*b*	*b*	*b*
BP86	**3ds**	1.032	0.948	0.012	48	0.2	**C1bD**	0.756	1.030	0.064	59	0.9
B3LYP		1.058	0.955	0.017	48	0.4		0.764	1.025	0.064	59	0.7
B3PW91		1.038	0.941	0.014	48	0.3		0.795	1.022	0.092	58	1.4
PBE0		1.034	0.936	0.014	48	0.3		0.829	1.021	0.118	58	1.8
TPSSh		1.022	0.925	0.012	48	0.2		0.760	1.020	0.066	59	0.8
M06-L		1.038	0.935	0.013	48	0.2		0.860	1.036	0.110	57	1.4
M06		1.066	0.963	0.019	48	0.4		0.843	1.026	0.119	58	2.0
BP86	**3sd**	1.048	0.958	0.014	48	0.2	**C2EB**	0.669	0.984	0.021	60	0.3
B3LYP		1.076	0.978	0.018	48	0.4		0.722	0.985	0.034	59	0.5
B3PW91		1.057	0.952	0.016	48	0.3		0.695	0.977	0.031	59	0.4
PBE0		1.056	0.947	0.017	48	0.3		0.699	0.974	0.033	59	0.5
TPSSh		1.039	0.935	0.015	48	0.2		0.686	0.975	0.026	59	0.3
M06-L		1.077	0.958	0.018	47	0.3		0.740	0.977	0.043	58	0.8
M06		1.116	1.000	0.028	48	0.7		0.729	0.982	0.044	59	0.9
BP86	**4sss**	1.049	0.960	0.014	48	0.2	**C2PG**	0.739	1.059	0.030	59	0.0
B3LYP		1.072	0.976	0.015	48	0.3		0.804	1.091	0.042	58	0.1
B3PW91		1.057	0.953	0.016	48	0.3		0.768	1.063	0.039	58	0.1
PBE0		1.052	0.945	0.017	48	0.3		0.769	1.057	0.041	58	0.1
TPSSh		1.039	0.935	0.015	48	0.3		0.749	1.051	0.034	59	0.1
M06-L		1.064	0.951	0.016	48	0.3		0.799	1.072	0.038	58	0.1
M06		1.095	0.983	0.024	48	0.6		0.772	1.060	0.039	58	0.1
BP86	**4dss**	1.014	0.930	0.013	48	0.2	**T1EB**	0.984	1.150	0.099	56	1.1
B3LYP		1.031	0.940	0.014	48	0.2		0.968	1.144	0.083	56	0.8
B3PW91		1.047	0.953	0.011	48	0.1		0.984	1.138	0.100	56	1.0
PBE0		1.020	0.915	0.014	48	0.3		0.985	1.133	0.105	56	1.1
TPSSh		1.029	0.934	0.011	48	0.1		0.943	1.138	0.073	57	0.7
M06-L		1.026	0.923	0.015	48	0.2		0.944	1.134	0.079	57	0.8
M06		1.047	0.943	0.019	48	0.4		1.039	1.132	0.151	56	1.9
BP86	**4sds**	1.026	0.963	0.007	49	0.0						
B3LYP		1.056	0.981	0.009	48	0.1						
B3PW91		1.036	0.959	0.008	48	0.0						
PBE0		1.029	0.954	0.008	48	0.0						
TPSSh		1.017	0.939	0.008	48	0.0						
M06-L		1.029	0.955	0.006	48	0.0						
M06		1.052	0.981	0.013	48	0.4						
BP86	**4ssd**	1.036	0.942	0.015	48	0.2						
B3LYP		1.053	0.951	0.015	48	0.2						
B3PW91		1.040	0.934	0.017	48	0.3						

DOI: 10.1021/acs.jpca.5b02041
J. Phys. Chem. A 2015, 119, 4993−5008

Table 6. continued

functional	system	$l_{H\cdots BCP}$	$l_{BCP\cdots Al}$	Δ_{ld}	$\%_{HM}$	$\Delta\%_{HM}$	system	$l_{H_a\cdots BCP}$	$l_{BCP\cdots M}$	Δ_{ld}	$\%_{HM}$	$\Delta\%_{HM}$
PBE0		1.037	0.929	0.018	48	0.3						
TPSSh		1.029	0.921	0.017	48	0.3						
M06-L		1.048	0.934	0.017	48	0.2						
M06		1.068	0.957	0.021	48	0.4						
BP86	**4dsd**	1.033	0.918	0.012	48	0.2						
B3LYP		1.038	0.941	0.015	48	0.2						
B3PW91		1.032	0.920	0.012	48	0.2						
PBE0		1.030	0.918	0.017	48	0.3						
TPSSh		1.022	0.912	0.016	48	0.3						
M06-L		1.048	0.926	0.018	47	0.3						
M06		1.067	0.947	0.021	47	0.4						

[a] $BP_{H\cdots C}$ instead of $BP_{H\cdots Al}$ has been obtained; see Figure 4. [b] $BP_{Co\cdots C_\gamma}$ instead of $BP_{Co\cdots H_\gamma}$ has been obtained.

particularly noticeable in the case of BCP of $H_a\cdots M$ agostic bonds (M06-based ranges of ε are 0.1−1.4 and 0.3−4.6 for IMCIHBs and ABs, respectively). As a consequence, it seems that one can distinguish IMCIHBs and ABs on the basis of ε values, which are either somewhat (PBE0) or considerably (M06) higher for the latter type of interaction. This finding, however, deserves further studies.

The other feature of systems with an agostic bond was to be the close proximity of $BCP_{H\cdots M}$ and RCP, i.e., a small value of the d_{br} distance.[27,28] As shown, however, e.g., in Figure 6 of ref 32 for a vanadium complex containing a γ-agostic bond this distance can be longer, showing that d_{br} may strongly depend on the type of an agostic bond and on the size of a quasi-ring. To check this possibility, we have also computed values of d_{br} and collected them in the right parts of Tables 4 and 5 for IMCIHBs and ABs, respectively. First of all, it is seen that these distances are indeed much lower in molecules with the small size of a quasi-ring. This conclusion is particularly evident for systems with IMCIHB. Molecules **2s** and **2d**, both possessing a five-membered quasi-ring, feature low values of d_{br} (0.63 and 0.79 Å, respectively), whereas molecules **3ss**, **3ds**, and **3sd**, all possessing a six-membered quasi-ring, have this parameter amounting to 1.22 Å. Even larger values of d_{br} (up to 1.81 Å for **4dss**) characterize IMCIHB systems with a seven-membered quasi-ring. In the case of the three molecules possessing a β-agostic bond (**C1EB**, **C2EB**, and **T1EB**) values of d_{br} are in the range of 0.21 Å (**T1EB**) to 0.64 Å (**C1EB**); thus they are well below the range for a five-membered quasi-ring formed by γ-agostic bonds (0.87 Å −1.11 Å) and the value of d_{br} in **C1bD** (1.12 Å) possessing a six-membered quasi-ring formed by a δ-agostic bond. A considerably lower value of d_{br} (0.21 Å) in addition to a larger ellipticity (1.3) obtained for **T1EB** ($C_2H_5TiCl_2^+$) in comparison with their counterparts (0.64 Å and 0.4, respectively) for **C1EB** ($C_2H_5CoCl_2^{2+}$) may indicate lesser stability of the former.

Comparing IMCIHB and AB systems possessing the same formal order of a quasi-ring, one can see that the d_{br} distance in **2s** and **2d** is shorter than in **C1PG**, **C1BG**, and **C2PG** (all these systems possess a five-membered quasi-ring), whereas d_{br} in **3ss**, **3ds**, and **3sd** (1.22 Å) is only somewhat greater than in **C1bD** (1.12 Å). The former likely results from the strained forms of five-membered quasi-rings in systems with IMCIHB.[3,4] Unfortunately, we cannot compare values of d_{br} obtained for four-membered quasi-ring AB systems **C1EB**, **C2EB**, and **T1EB** with also four-membered quasi-ring system **1** because **1** does not feature $BCP_{H\cdots Al}$. As a result of this analysis, it is concluded that systems with IMCIHB can hardly be distinguished from systems with agostic bonds merely on the basis of the d_{br} distance. Further studies on larger group of systems, particularly those with IMCIHB forming a four-membered quasi-ring traced by a bond path and a concomitant bond critical point and ε-agostic bonds would be, however, helpful to assess the validity of this conclusion.

On the contrary, on considering ρ_r and $\Delta\rho_{br}$ one can see that, in general, both these parameters are considerably greater in systems with agostic bonds. For instance, values of ρ_r are from 0.008 au in **4sds** to 0.023 au in **2s**, whereas in the case of systems with AB ρ_r amounts to 0.029 au (**C1bD**) to 0.080 au (**C1EB**). This result shows that, in the case of systems with an agostic bond, the electron density is considerably drawn into the interior of the quasi-ring. As a consequence, it seems that values of ρ_r (and in a lesser extent of $\Delta\rho_{br}$) may help to distinguish IMCIHBs and ABs.

The other property that has recently been studied and yielded reliable distinction between IMCIHBs and ABs is the curvature of the H···Al and H···M bond paths.[1] This issue will be discussed in the next paragraph.

Curvatures of Bond Paths. To investigate curvatures of H···Al and H···M bond paths we have computed values of differences between their lengths and H···M (M = Al, Co, Ti) distances (Δ_{ld}) as well as two geometric descriptors of the bond path distortion, introduced earlier by Tognetti et al.:[30]

$$\%_{HM} = 100\frac{d_{BCP\cdots M}}{d_{H\cdots M}} \quad (1)$$

$$\Delta\%_{HM} = 100\left(\frac{d_{H\cdots BCP} + d_{BCP\cdots M}}{d_{H\cdots M}} - 1\right) \quad (2)$$

The former describes the BCP···M distance relative to the H···M distance, and the latter is a measure of the displacement of the BCP relative to the line connecting the pair of interacting atoms. For a perfectly straight bond path one gets $\Delta\%_{HM} = 0$. Values of these parameters as well as lengths of H···BCP ($l_{H\cdots BCP}$) and BCP···M ($l_{BCP\cdots M}$) fragments of the H···M bond paths are listed in Table 6.

One can see that *all* functionals (but B3LYP in **2s**) show that $l_{H\cdots BCP} > l_{BCP\cdots Al}$ for IMCIHBs, whereas the opposite relation holds for ABs, i.e., $l_{H\cdots BCP} < l_{BCP\cdots M}$. As a consequence, in the case of systems with IMCIHB, the relevant bond critical point is somewhat closer to the metal atom (Al), whereas, in the case of systems with agostic bonds, this bond critical point is, instead, significantly closer to the agostic hydrogen.[27,28,30] This conclusion is supported by values of $\%_{HM}$ that, in the case of

DOI: 10.1021/acs.jpca.5b02041
J. Phys. Chem. A 2015, 119, 4993−5008

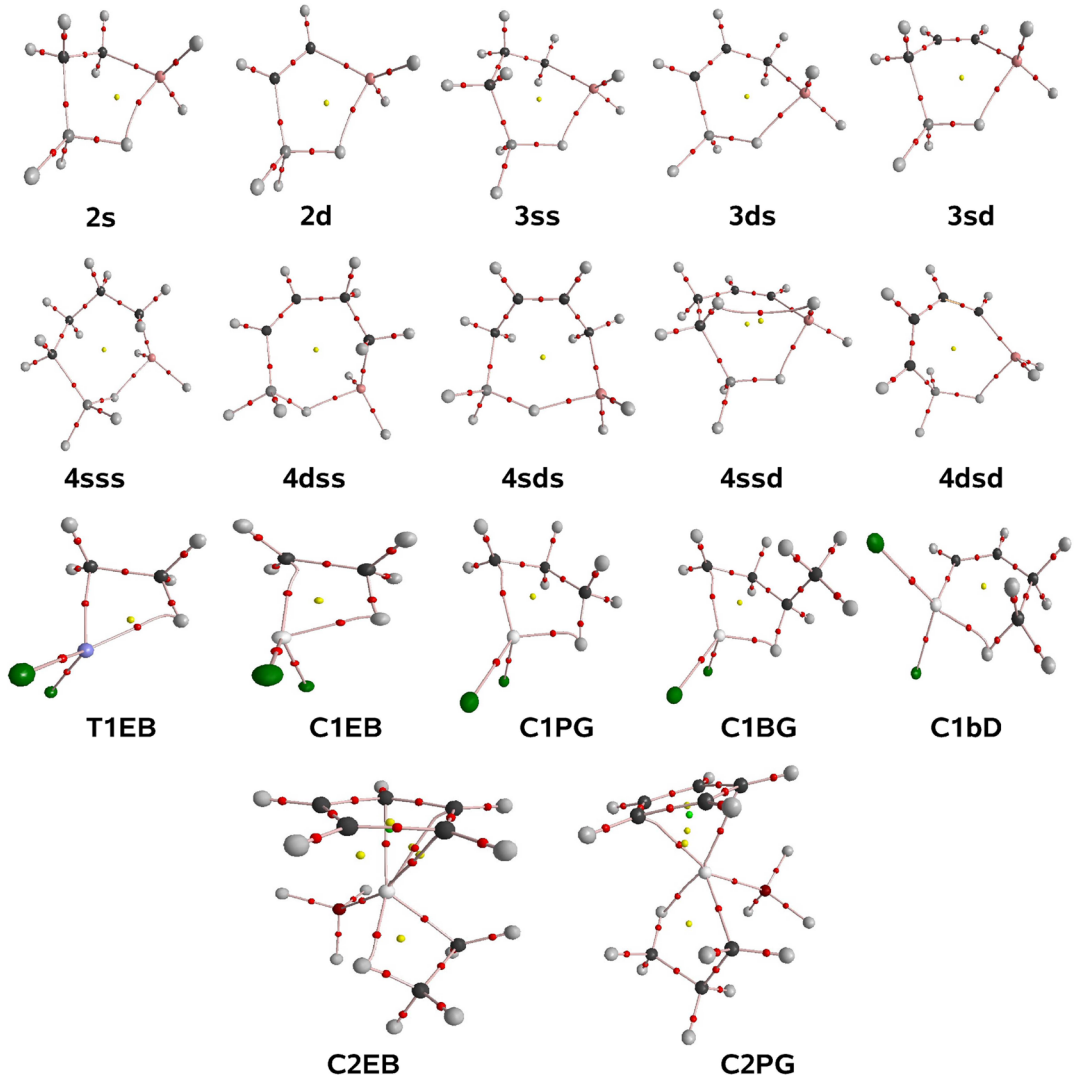

Figure 3. Molecular graphs of investigated model systems with either intramolecular charge-inverted hydrogen bonds or agostic bonds. Bond critical points are shown by red balls and ring critical points by yellow balls.

intramolecular charge-inverted hydrogen bonds, are somewhat lower than 50 (47−48), whereas, in the case of systems with agostic bonds, these values are clearly greater than 50 (56−61). An even wider range of $\%_{HM}$ (55−69) has been obtained by Tognetti et al.[30] in their studies on complexes with agostic bonds. If PBE0-based values of Δ_{ld} are taken into account only, one can see that, although they overlap due to high value of Δ_{ld} for the **2s** system (0.063 Å), the range of Δ_{ld} values for agostic bonds (0.031−0.118 Å) is shifted toward greater values relative to the range of Δ_{ld} for IMCIHBs (0.008−0.063 Å). This result clearly indicates that bond paths tracing agostic bonds are considerably more curved than bond paths for intramolecular charge-inverted hydrogen bonds. This is, however, not so clearly evident if values of $\Delta\%_{HM}$ are investigated instead, because ranges of $\Delta\%_{HM}$ are similar to each other (0.0−2.1 and 0.1−2.2 for IMCIHBs and ABs, respectively). Nevertheless, it should be underlined that Δ_{ld} is a better measure of the curvature of a bond path than $\Delta\%_{HM}$ because the former directly takes into account the length of a bond path and, moreover, compares it with the H···M distance. One should also mention that the PBE0-based range of $\Delta\%_{HM}$ values obtained for agostic systems was even wider (0−6) in studies of Tognetti et al.[30] Interestingly, in the case of agostic bonds, minimal and maximal values of $\Delta\%_{HM}$ do not go in pair with minimal and maximal values of Δ_{ld}. The former are the greatest and the lowest for **C1PG** (2.2) and **C2PG** (0.1), respectively, whereas Δ_{ld} is the greatest in **C1bD** (0.118 Å) and the lowest in **C1EB** (0.031 Å). One should stress, however, that both these parameters, in fact, measure somewhat different properties of the H···M bond path. Namely, Δ_{ld} measures the real difference between the length of the bond path and the H···M distance, whereas, on the contrary, $\Delta\%_{HM}$ measures the displacement of the BCP relative to the line connecting the two interacting atoms. Of course, it is the former parameter that is a better measure of the curvature of a bond path.

Even more direct insight into curvatures of $BP_{H\cdots Al}$ and $BP_{H\cdots M}$ can be obtained by looking at molecular graphs; these are shown in Figure 3. In the case of molecular graphs representing systems with IMCIHB, the H···Al bond paths are rather straight; however, in the case of **2s**, **2d**, and **3ss**, i.e., instances possessing smaller sized quasi-ring, the concavity of $BP_{H\cdots Al}$ toward RCP can easily be noticed. On the contrary, in the case of systems with agostic bonds, one obtains $BP_{H\cdots M}$ being straight in the M···BCP section, whereas it is highly curved in the closest proximity of the agostic hydrogen. The considerably large curvature of the M···H bond path near the

DOI: 10.1021/acs.jpca.5b02041
J. Phys. Chem. A 2015, 119, 4993−5008

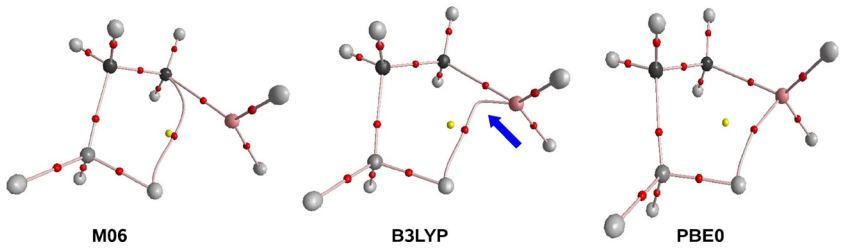

Figure 4. Molecular graphs of $H_3SiCH_2CH_2AlH_2$ (**2s**) obtained by means of M06 (left), B3LYP (center), and PBE(0) exchange−correlation functionals. Bond critical points are shown by red balls and ring critical points by yellow balls. The blue arrow points the considerably large curvature of the H···Al bond path.

agostic hydrogen in some systems possessing agostic bonds has also been reported by others.[27,28,30] This difference in curvatures of H···M bond paths is so far the most important difference between agostic bonds and intramolecular charge-inverted hydrogen bonds that gives the opportunity to distinguish these two types of interactions on the basis of the topology of the electron density distribution.

We note that the described difference in curvatures of H···Al and H···M bond paths may even be enhanced if other than PBE0 exchange−correlation functional is used. For example, Figure 4 displays molecular graphs of **2s** obtained by means of M06 (left), B3LYP (center), and PBE0 (right). Similarly as for H···M bond paths tracing agostic bonds (see the lowest two rows in Figure 3), the H···Al bond path in **2s** is highly curved. Whereas PBE0 shows a bow-like shape of this path, a very large curvature of $BP_{H\cdots Al}$ has been obtained by means of B3LYP (Δ_{ld} = 0.488 Å and $\Delta\%_{HM}$ = 8.4). Importantly, one should notice, however, that, contrary to agostic bonds, in this case this curvature is (see the blue arrow in Figure 4) located near the metal (aluminum) atom instead of hydrogen. A very small d_{br} distance obtained by means of B3LYP (0.32 Å) in comparison with PBE0 (0.63 Å) is connected with low λ_2 value, i.e., the curvature in the direction of RCP, and the negligible value of $\Delta\rho_{br}$ (Table 4). By the way, we also pay attention to the molecular graph of **2s** obtained by means of M06 (Figure 4). Instead of a bond path to the aluminum atom, one obtains a H···C bond path that should, however, rather be regarded as an artifact of the use of M06 as the presence of IMCIHB in **2s** is unarguable.[3,4] The tendency of M06 to create a bond path to a carbon has already been mentioned earlier and is evidenced in **C1BG**.

At the end of QTAIM-based analysis we point out the significant curvature of the $C_\alpha\cdots M$ bond path near the α-carbon in some systems with agostic bonds. A similar finding has already been described by Scherer et al.[27] and proposed to be a more general criterion for identifying the presence of an agostic bond. This curvature of $BP_{C_\alpha\cdots M}$ can, however, be easily noticed (Figure 3) in **C1PG**, **C1BG**, and particularly in **C1EB**, but not in molecules **T1EB**, **C1bD**, **C2EB**, and **C2PG**. Moreover, as clearly seen from Figure 1b in ref 27, the curvature of $BP_{C_\alpha\cdots M}$ is much more modest than that of $BP_{H_\beta\cdots M}$, particularly in the vicinity of the agostic hydrogen.

CONCLUSIONS

We have performed geometrical and QTAIM-based comparison between H···Al intramolecular charge-inverted hydrogen bonds (IMCIHB) and H···M (M = Ti, Co) α-, β-, γ-, and δ-agostic bonds (AB). Because it is known that both values of QTAIM parameters and molecular graphs may depend on a choice of an exchange−correlation functional, we have taken care of studying the influence of the exchange−correlation functional on QTAIM-based characteristics of investigated model systems. Therefore, our calculations have been performed using seven DFT functionals (BP86, B3LYP, B3PW91, PBE0, TPSSh, M06-L, M06). It turned out that our model systems reveal agostic bonds that are "stable" due to the permanent presence of the $M\cdots H_a$ bond path irrespective of the choice of the exchange−correlation functional. One of our main purposes was then to study the influence of investigated functionals on geometrical and QTAIM-based (computed at BCP and RCP) parameters relevant to both types of interactions. We have found that (i) BP86 yields the longest either Si−H or C−H bonds, whereas M06-L and M06 tend to give them the shortest, (ii) M06 and B3LYP tend to give longer H···Al distances and TPSSh tends to give them the shortest, (iii) M06-L and M06 tend to give longer $H_a\cdots M$ distances, (iv) PBE0 and M06 may lead to the shortest $C_a\cdots M$ distances, (v) TPSSh and, to a somewhat lesser extent, BP86 give the best values of geometrical parameters in comparison to experimental data, (vi) formation of an agostic bond leads to a significant elongation of the C−H bond participating in AB, (vii) the $H_a\cdots M$ distance is the shortest in the case of β-agostic bond, and (viii) IMCIHBs are longer than ABs if α-agostic bonds are excluded.

If QTAIM-based parameters computed at either $BCP_{H\cdots Al}$ or $BCP_{H\cdots M}$ have been considered, then it has been concluded that, in general, a choice of the exchange−correlation functional has a negligible influence on values of the electron density (ρ_b) and the electronic total energy density (H_b). Some more noticeable effects have only been found in the case of the Laplacian of the electron density ($\nabla^2\rho_b$), all curvatures (particularly in the direction of bonding atoms (λ_3) and, additionally in the case of systems with an agostic bond, in the direction of the ring critical point, λ_2), and the bond ellipticity (ε).

We have shown that both IMCIHBs and ABs feature positive values of $\nabla^2\rho_b$ and negative values of H_b. Thus, in spite of the fact that agostic bonds are commonly characterized as closed-shell interactions, similarly as IMCIHBs, they also can possess some covalent character. As a consequence, one cannot distinguish IMCIHBs and agostic bonds on the basis of the sign of H_b. On the contrary, it seems, however, that one can distinguish IMCIHBs and ABs on the basis of ε values that are either somewhat (PBE0) or considerably (M06) higher for the latter type of interaction. Significantly greater values of ε together with greater values of ρ_r obtained for systems with an agostic bond show that the electron density is drawn into the interior of a quasi-ring. As a consequence, values of ρ_r may be helpful in distinguishing IMCIHBs and ABs.

DOI: 10.1021/acs.jpca.5b02041
J. Phys. Chem. A 2015, 119, 4993−5008

An additional distinction between IMCIHB and AB is provided by an insightful examination of H···Al and H···M bond paths. Namely, we have shown that, in the case of systems with IMCIHB, $BCP_{H\cdots Al}$ is somewhat closer to the metal atom (Al), whereas, in the case of systems with AB, $BCP_{H\cdots M}$ is, instead, significantly closer to the agostic hydrogen. This result has been shown to be independent of the exchange−correlation functional. A further difference between the IMCIHB and agostic bond is in curvatures of bond paths tracing these interactions. We have shown that bond paths tracing agostic bonds are considerably more curved than bond paths for intramolecular charge-inverted hydrogen bonds. After more detailed studies on the curvatures of these bond paths we have concluded that agostic bonds are characterized by H···M bond paths being straight in the M···BCP section and highly curved near the agostic hydrogen. On the contrary, in the case of molecular graphs representing IMCIHB, the H···Al bond path is rather straight. Its somewhat bow-like shape with the concavity of $BP_{H\cdots Al}$ toward RCP can, however, be found in systems with a smaller sized quasi-ring. Importantly, any substantial curvature in the vicinity of hydrogen is not present. Quite the contrary, significant curvature near the metal atom (Al) can be obtained, e.g., if the B3LYP exchange−correlation functional is used instead of PBE0. As a consequence, this fact even further highlights the ability to distinguish IMCIHBs and ABs on the basis of their molecular graphs. It has also been shown that M06 fails to predict the unarguable presence of IMCIHB in $H_3SiCH_2CH_2AlH_2$.

AUTHOR INFORMATION

Corresponding Author

*Phone: +48 (56) 6114695. Fax: +48 (56) 6542477. E-mail: teojab@chem.uni.torun.pl.

Notes

The authors declare no competing financial interest.

ACKNOWLEDGMENTS

Calculations have been carried out on the multiprocessor cluster at the Interdisciplinary Centre for Mathematical and Computational Modelling (ICM) at the University of Warsaw thanks to the G50-10 grant.

REFERENCES

(1) Jabłoński, M. Charge-Inverted Hydrogen Bond vs. Other Interactions Possessing a Hydridic Hydrogen Atom. *Chem. Phys.* **2014**, *433*, 76−84.

(2) Jabłoński, M. Binding of X-H to the Lone-Pair Vacancy: Charge-Inverted Hydrogen Bond. *Chem. Phys. Lett.* **2009**, *477*, 374−376.

(3) Jabłoński, M. Intramolecular Charge-Inverted Hydrogen Bond. *J. Mol. Struct. (THEOCHEM)* **2010**, *948*, 21−24.

(4) Jabłoński, M. Full vs. Constrain Geometry Optimization in the Open-Closed Method in Estimating the Energy of Intramolecular Charge-Inverted Hydrogen Bonds. *Chem. Phys.* **2010**, *376*, 76−83.

(5) Jabłoński, M. Theoretical Insight into the Nature of the Intermolecular Charge-Inverted Hydrogen Bond. *Comput. Theor. Chem.* **2012**, *998*, 39−45.

(6) Jabłoński, M.; Sokalski, W. A. Physical Nature of Interactions in Charge-Inverted Hydrogen Bonds. *Chem. Phys. Lett.* **2012**, *552*, 156−161.

(7) Brookhart, M.; Green, M. L. H. Carbon-Hydrogen-Transition Metal Bonds. *J. Organomet. Chem.* **1983**, *250*, 395−408.

(8) Brookhart, M.; Green, M. L. H.; Wong, L. L. Carbon-Hydrogen-Transition Metal Bonds. *Prog. Inorg. Chem.* **1988**, *36*, 1−124.

(9) Brookhart, M.; Green, M. L. H.; Parkin, G. Coordination Chemistry of Saturated Molecules Special Feature - Review. *Proc. Natl. Acad. Sci. U. S. A.* **2007**, *104*, 6908−6914.

(10) Robertson, A. H. J.; McQuillan, P.; McKean, D. C. Carbon-Hydrogen Bond Properties and Alkyl Group Geometries in Dichloro-(η^5-cyclopentadientyl)-methyltitanium(IV) and Dichloro(η^5-cyclopentadienyl)-ethyltitanium(IV) [$TiR(\eta^5\text{-}C_5H_5Cl_2$] (R = Me or Et). *J. Chem. Soc., Dalton Trans.* **1995**, 3941−3953.

(11) Han, Y.; Deng, L.; Ziegler, T. A Density Functional Study of β-Hydride and Methyl Migratory Insersion in $CpM(PH_3)(CH_2CH_2)R^+$ (M = Co, Rh, Ir; R = H, CH_3). *J. Am. Chem. Soc.* **1997**, *119*, 5939−5945.

(12) Haaland, A.; Scherer, W.; Ruud, K.; McGrady, G. S.; Downs, A. J.; Swang, O. On the Nature and Incidence of β-Agostic Interactions in Ethyl Derivatives of Early Transition Metals: Ethyltitanium Trichloride and Related Compounds. *J. Am. Chem. Soc.* **1998**, *120*, 3762−3772.

(13) McGrady, G. S.; Downs, A. J. Molecules With Hydride or Alkyl Ligands and Including d^0 Transition Metal Centers: Problem Cases for the Simple VSEPR Model. *Coord. Chem. Rev.* **2000**, *197*, 95−124.

(14) Clot, E.; Eisenstein, O. Agostic Interactions from a Computational Perspective: One Name, Many Interpretations. *Struct. Bonding (Berlin)* **2004**, *113*, 1−36.

(15) Scherer, W.; McGrady, G. S. Agostic Interactions in d^0 Metal Alkyl Complexes. *Angew. Chem., Int. Ed.* **2004**, *43*, 1782−1806.

(16) Lein, M. Characterization of Agostic Interactions in Theory and Computation. *Coord. Chem. Rev.* **2009**, *253*, 625−634.

(17) Schneider, J. J.; Si-H, C.-H. Activation by Transition Metal Complexes: A Step Towards Isolable Alkane Complexes? *Angew. Chem., Int. Ed. Engl.* **1996**, *35*, 1068−1075.

(18) Lin, Z. Structural and Bonding Characteristics in Transition Metal-Silane Complexes. *Chem. Soc. Rev.* **2002**, *31*, 239−245.

(19) Braga, D.; Grepioni, F.; Biradha, K.; Desiraju, G. R. Agostic Interactions in Organometallic Compounds. A Cambridge Structural Database Study. *J. Chem. Soc., Dalton Trans.* **1996**, 3925−3930.

(20) Beswick, M. A.; Wright, D. S. Synthetic Applications of p Block Metal Dimethylamido Reagents. *Coord. Chem. Rev.* **1998**, *176*, 373−406.

(21) Demachy, I.; Volatron, F. π-Bond vs. Agostic Interaction in Three-Coordinated Alkoxy and Thiolate Derivatives of Aluminium, Boron and Cationic Carbon - An ab Initio Study of $H_2X\text{-}YR$ Systems (X = Al, B, C^+; Y = O, S; R = H, CH_3). *Eur. J. Inorg. Chem.* **1998**, 1015−1023.

(22) Scheins, S.; Messerschmidt, M.; Gembicky, M.; Pitak, M.; Volkov, A.; P, C.; Harvey, B. G.; Turpin, G. C.; Arif, A. M.; Ernst, R. D. Charge Density Analysis of the (C-C)→Ti Agostic Interactions in a Titanacyclobutane Complex. *J. Am. Chem. Soc.* **2009**, *131*, 6154−6160.

(23) McNaught, A. D., Wilkinson, A. *IUPAC Compendium of Chemical Terminology (The Gold Book)*; Blackwell Scientific Publications: Oxford, U.K., 1997.

(24) Bader, R. F. W. *Atoms in Molecules: A Quantum Theory*; Oxford University Press: New York, 1990.

(25) Popelier, P. L. A. *Atoms in Molecules. An Introduction*; Longman: Singapore, 2000.

(26) Matta, C. F.; Boyd, R. J. *The Quantum Theory of Atoms in Molecules*; Wiley-VCH: Weinheim, 2007.

(27) Scherer, W.; Hieringer, W.; Spiegler, M.; Sirsch, P.; McGrady, G. S.; Downs, A. J.; Haaland, A.; Pedersen, B. Characterisation of Agostic Interactions by a Topological Analysis of Experimental and Theoretical Charge Densities in [$EtTiCl_3$(dmpe)] [dmpe = 1,2-bis(dimethylphosphino)ethane]. *Chem. Commun.* **1998**, 2471−2472.

(28) Popelier, P. L. A.; Logothetis, G. Characterization of an Agostic Bond on the Basis of the Electron Density. *J. Organomet. Chem.* **1998**, *555*, 101−111.

(29) Vidal, I.; Melchor, S.; Alkorta, I.; Elguero, J.; Sundberg, M. R.; Dobado, J. A. On the Existence of α-Agostic Bonds: Bonding Analyses of Titatium Alkyl Complexes. *Organometallics* **2006**, *25*, 5638−5647.

(30) Tognetti, V.; Joubert, L.; Raucoules, R.; De Bruin, T.; Adamo, C. Characterizing Agosticity Using the Quantum Theory of Atoms in

DOI: 10.1021/acs.jpca.5b02041
J. Phys. Chem. A 2015, 119, 4993−5008

Molecules: Bond Critical Points and Their Local Properties. *J. Phys. Chem. A* **2012**, *116*, 5472−5479.
(31) Tognetti, V.; Joubert, L.; Cortona, P.; Adamo, C. Toward a Combined DFT/QTAIM Description of Agostic Bonds: The Critical Case of a Nb(III) Complex. *J. Phys. Chem. A* **2009**, *113*, 12322−12327.
(32) Tognetti, V.; Joubert, L. On the Influence of Density Functional Approximations on Some Local Bader's Atoms-in-Molecules Properties. *J. Phys. Chem. A* **2011**, *115*, 5505−5515.
(33) Bühl, M.; Kabrede, H. Geometries of Transition-Metal Complexes from Density-Functional Theory. *J. Chem. Theory Comput.* **2006**, *2*, 1282−1290.
(34) Pantazis, D. A.; McGrady, J. E.; Maseras, F.; Etienne, M. Critical Role of the Correlation Functional in DFT Descriptions of an Agostic Niobium Complex. *J. Chem. Theory Comput.* **2007**, *3*, 1329−1336.
(35) Pantazis, D. A.; McGrady, J. E.; Besora, M.; Maseras, F.; Etienne, M. On the Origin of α- and β-Agostic Distortions in Early-Transition-Metal Alkyl Complexes. *Organometallics* **2008**, *27*, 1128−1134.
(36) Jensen, F. *Introduction to Computational Chemistry*; John Wiley & Sons Ltd.: Chichester, U.K., 1999.
(37) Zhao, Y.; Truhlar, D. G. The M06 Suite of Density Functionals For Main Group Thermochemistry, Thermochemical Kinetics, Noncovalent Interactions, Excited States, and Transition Elements: Two New Functionals and Systematic Testing of Four M06-Class Functionals and 12 Other Functionals. *Theor. Chem. Acc.* **2008**, *120*, 215−241.
(38) Koch, W., Holthausen, M. C. *A Chemist's Guide to Density Functional Theory*; Viley-VCH: Weinheim, 2001.
(39) Becke, A. D. Density-Functional Exchange-Energy Approximation With Correct Asymptotic-Behavior. *Phys. Rev. A* **1988**, *38*, 3098−3100.
(40) Perdew, J. P. Density-Functional Approximation for the Correlation Energy of the Inhomogeneous Electron Gas. *Phys. Rev. B* **1986**, *33*, 8822−8824.
(41) Becke, A. D. Density-Functional Thermochemistry. III. The Role of Exact Exchange. *J. Chem. Phys.* **1993**, *98*, 5648−5652.
(42) Lee, C.; Yang, W.; Parr, R. G. Development of the Colle-Salvetti Correlation-Energy Formula into a Functional of the Electron Density. *Phys. Rev. B* **1988**, *37*, 785−789.
(43) Perdew, J. P. In *Electronic Structure of Solids*; Ziesche, P., Eschrig, H., Eds.; Akademie Verlag: Berlin, 1991.
(44) Perdew, J. P.; Chevary, J. A.; Vosko, S. H.; Jackson, K. A.; Pederson, M. R.; Singh, D. J.; Fiolhais, C. Atoms, Molecules, Solids, and Surfaces: Applications of the Generalized Gradient Approximation for Exchange and Correlation. *Phys. Rev. B* **1992**, *46*, 6671−6687.
(45) Perdew, J. P.; Burke, K.; Ernzerhof, M. Generalized Gradient Approximation Made Simple. *Phys. Rev. Lett.* **1996**, *77*, 3865−3868.
(46) Perdew, J. P.; Burke, K.; Ernzerhof, M. Errata: Generalized Gradient Approximation Made Simple. *Phys. Rev. Lett.* **1997**, *78*, 1396.
(47) Adamo, C.; Barone, V. Toward Reliable Density Functional Methods Without Adjustable Parameters: The PBE0Model. *J. Chem. Phys.* **1999**, *110*, 6158−6170.
(48) Tao, J. M.; Perdew, J. P.; Staroverov, V. N.; Scuseria, G. E. Climbing the Density Functional Ladder: Nonempirical Meta-Generalized Gradient Approximation Designed for Molecules and Solids. *Phys. Rev. Lett.* **2003**, *91*, 146401−146404.
(49) Zhao, Y.; Truhlar, D. G. A New Local Density Functional for Main-Group Thermochemistry, Transition Metal Bonding, Thermochemical Kinetics, and Noncovalent Interactions. *J. Chem. Phys.* **2006**, *125*, 194101.
(50) Dunning, T. H., Jr. Gaussian Basis Sets for Use in Correlated Molecular Calculations. I. The Atoms Boron Through Neon and Hydrogen. *J. Chem. Phys.* **1989**, *90*, 1007−1023.
(51) Woon, D. E.; Dunning, T. H., Jr. Gaussian Basis Sets for Use in Correlated Molecular Calculations. III. The Atoms Aluminum Through Argon. *J. Chem. Phys.* **1993**, *98*, 1358−1371.
(52) Balabanov, N. B.; Peterson, K. A. Systematically Convergent Basis Sets for Transition Metals. I. All-Electron Correlation Consistent Basis Sets for the 3d Elements Sc-Zn. *J. Chem. Phys.* **2005**, *123*, 064107.
(53) Balabanov, N. B.; Peterson, K. A. Basis Set Limit Electronic Excitation Energies, Ionization Potentials, and Electron Affinities for the 3d Transition Metal Atoms: Coupled Cluster and Multireference Methods. *J. Chem. Phys.* **2006**, *125*, 074110.
(54) Jabłoński, M.; Palusiak, M. Basis Set and Method Dependence in Atoms in Molecules Calculations. *J. Phys. Chem. A* **2010**, *114*, 2240−2244.
(55) Jabłoński, M.; Palusiak, M. Basis Set and Method Dependence in Quantum Theory of Atoms in Molecules Calculations for Covalent Bonds. *J. Phys. Chem. A* **2010**, *114*, 12498−12505.
(56) Frisch, M. J.; Trucks, G. W.; Schlegel, H. B.; Scuseria, G. E.; Robb, M. A.; Cheeseman, J. R.; Scalmani, G.; Barone, V.; Mennucci, B.; Petersson, G. A.; et al. *Gaussian 09*; Gaussian, Inc.: Wallingford, CT, 2010.
(57) Biegler-König, F. W. *AIM2000 program*; University of Applied Sciences: Bielefeld, Germany, 2000.
(58) Cremer, D.; Kraka, E.; Slee, T. S.; Bader, R. F. W.; Lau, C. D. H.; Nguyen-Dang, T. T.; MacDougall, P. J. Description of Homoaromaticity in Terms of Electron Distributions. *J. Am. Chem. Soc.* **1983**, *105*, 5069−5075.

DOI: 10.1021/acs.jpca.5b02041
J. Phys. Chem. A 2015, 119, 4993−5008